12-2023

Early Pliocene Mice and Rats from the Gray Fossil Site of Eastern Tennessee: Implications for the Evolution of Cricetidae and Understanding of the Past Ecosystem

Ziqi Xu
East Tennessee State University

Early Pliocene Mice and Rats from the Gray Fossil Site of Eastern Tennessee: Implications for the Evolution of Cricetidae and Understanding of the Past Ecosystem

---

A thesis

presented to

the faculty of the Department of Geosciences

East Tennessee State University

In partial fulfillment

of the requirements for the degree

Master of Science in Geosciences

---

by

Ziqi (Stokke) Xu

December 2023

Dr. Joshua X. Samuels, Chair

Dr. Blaine W. Schubert

Dr. Steven C. Wallace

Keywords: cricetid, character state analysis, *Neotomodon*, *Postcopemys*, *Xenomys*

ABSTRACT

Early Pliocene Mice and Rats from the Gray Fossil Site of Eastern Tennessee: Implications for the Evolution of Cricetidae and Understanding of the Past Ecosystem

by

Ziqi (Stokke) Xu

Cricetidae ranks as the second-most species-rich and abundant mammalian family, with limited studies on eastern North American records prior to the Pleistocene. While cricetids has been previously noted at the early Pliocene Gray Fossil Site (GFS), this study provides a detailed description of eight taxa: *Postcopemys* (two species), *Symmetrodontomys*, Oryzomyini, *Peromyscus*, *Neotoma*, *Neotomodon*, and *Xenomys*. *Postcopemys* is the most common cricetid taxon at GFS, followed by *Peromyscus* and *Neotoma*. These records expand the stratigraphic and geographic range of multiple genera. Distinctive morphological features of GFS taxa suggest presence of several new species. The GFS cricetid assemblage exhibits diverse body sizes and dietary preferences, setting GFS apart from other contemporaneous sites and emphasizing its spatial and temporal uniqueness. The Appalachian region represents a biodiversity hotspot today, and GFS was likely an important habitat for cricetid evolution during the Pliocene.

ACKNOWLEDGEMENTS

I extend my sincere gratitude to my advisor, Dr. Joshua X. Samuels, and my committee members for providing unwavering guidance and invaluable advice throughout my academic journey. The commitment of the field and prep lab crews, along with the efforts of dedicated volunteers who diligently cleaned and picked out fossil materials, played an essential role in the success of my research. Special thanks to Keila Bredehoeft for her meticulous attention to cleaning my specimens, and to the collection crews for their exceptional care of the specimens throughout every stage of my research. Furthermore, I express heartfelt appreciation to my partner, Corinthas White III, and cherished friends like Feng Liang for their immersive emotional support. I am equally grateful to my family for their enduring belief in me and their crucial financial assistance over the years. The abundance of love and support from those around me has been instrumental in empowering me to pursue and achieve success in my academic endeavors.

TABLE OF CONTENTS

LIST OF TABLES

LIST OF FIGURES

CHAPTER 1. INTRODUCTION

The Late Neogene witnessed significant changes in climate and ecosystems. Grassland expanded and became the dominant ecosystem in western and central North America (Graham 1999; Edwards et al. 2010; Stromberg 2011), while woodlands and forests were only sparsely documented by a few terrestrial sites in eastern North America (DeSantis and Wallace 2008; Baskin and Baskin 2016; Ochoa et al. 2016). The Gray Fossil Site (GFS) in northeastern Tennessee stands out as one of these rare woodland sites and is additionally unique due to its sinkhole environment (Wallace and Wang 2004). The paleo-sinkhole fill at GFS mainly consists of silty-clay lacustrine rhythmites (Shunk et al. 2009); both graded and laminated lacustrine facies contain abundant terrestrial organic matter and record primarily warmer and wetter climatic intervals during sedimentation (DeSantis and Wallace 2008; Wallace 2011). This low-energy sedimentary environment has preserved a wealth of vertebrae fossils, among which are some uncommon taxa in the southeast. The discovery of an alligator, lizards, peccaries, red pandas, rhinos, tapirs, mastodon, and wolverine (Hulbert et al. 2009; Wallace 2011; Mead et al. 2012; Keenan and Annette 2017; Doughty et al. 2018; Samuels et al. 2018; Short et al. 2019) further suggests that GFS had a distinct paleoecosystem that once hosted fauna with diverse habitat preferences.

Cricetids, which are small rodents with mouse- or rat-like appearance, have a robust fossil record in North America. The earliest known North America cricetid, *Eumys*, dates back to the late Eocene (Lindsay 2008) and shares morphological similarities with certain Eurasian counterparts, suggesting a potential immigration or descendant relationship (Martin 1980, Lindsay 2008). Despite being less discussed than many other groups, Cricetidae is the second-most species-rich family of mammals and was among the most widespread and diverse clades in

the Late Cenozoic (Steppan et al. 2004; Fabre et al. 2012). North America alone boasted 62 genera and 262 species during this time (Samuels and Hopkins 2017). Phylogenetic analysis using morphological characters and molecular markers further reveals major radiation and dispersal events of cricetids in the Late Neogene of North America (e.g., Martin, Goodwin et al. 2002; Martin, Honey et al. 2002; Martin et al. 2008, 2018, 2019; Korth 2011; Mou 2011; Fabre et al. 2012; Kelly and Whistler 2014; Martin and Zakrzewski 2019; Kelly and Martin 2022; Kelly et al. 2022). Many late Miocene and early Pliocene cricetids with advanced traits and ties to extant taxa flourished in the western and central United States (Kelly and Martin 2022). Their opportunistic dietary habits and high reproductive rate enable them to quickly colonize and adapt to new geographic areas. As one of the most speciose families of rodents, Cricetidae plays an indispensable role in ecosystems as a primary food resource for numerous carnivorous predators (e.g., Lindsay 2008; Martínez-Chapital et al. 2017).

New World rats and mice are characterized by specific dental features, generally including one incisor and three molars on each side of the maxilla and dentary (Carleton and Musser 1984, Nowak 1999, Lindsay 2008). The dental morphology, number of roots, and presence of accessory structures vary among genera and usually can be used to as markers with phylogenetic significance to differentiate them. For instance, although the upper molars generally have three roots and the lowers have two, accessory rootlets are frequently spotted on more derived taxa like Sigmodontinae and Neotominae in South and North America (Korth 1998, Lindsay 2008, Kelly and Whistler 2014, Ronez et al. 2021). The anterocone(id) on the anterior molar could be reduced or lost on the middle and posterior molars in certain derived genera (Lindsay 2008). More advanced genera also tend to have a relatively small third molar where the posterior cusp(id)s are reduced in size and shape. Compared to hypsodont clade which

tends to have prismatic, lophodont-like, and rootless dentition specialized for more herbivore diet, small brachydont cricetids are prone to retain accessory structures and pointy main cusp(id)s to accommodate to an insectivorous or omnivorous diet (Lindsay 2008, Lindsay and Whistler 2014). These features can provide insights into the dietary preferences and adaptations of these rodents. Studying Cricetidae through fossil dental records not only sheds light on their evolutionary history and distribution but also unveils the unique paleoecological settings preserved in different regions of the Americas.

While the field crew has been actively collecting all macro- and microfossil materials from GFS over the years, research efforts have predominantly focused on larger mammals and various reptiles (e.g., DeSantis and Wallace 2008; Hulbert et al. 2009; Boardman and Schubert 2011; Wallace 2011; Bourque and Schubert 2015; Jasinski and Moscato 2017; Doughty et al. 2018). While small mammals like cricetids have received extensive attention elsewhere (e.g., Martin, Goodwin et al. 2002; Martin, Honey et al. 2002; Martin et al. 2008, 2018, 2019; Korth 2011; Mou 2011; Kelly and Whistler 2014), they haven't been studied yet at GFS. Only a few cricetids genera have been mentioned in previous research to support taxonomic diversity and the age range reconstruction of the site (Samuels et al. 2018). With the ongoing excavation and screen-washing at GFS and the growing number of cricetid specimens being added to the collection, there is a need for a systematic analysis of this rodent group.

GFS stands out as one of the few pre-Pleistocene records of cricetids in eastern North America. Other Pliocene-age sites are limited to Pipe Creek Sinkhole in Indiana and a few sites (e.g., Inglis 1A, 1C; Haile 15A) in Florida (Ruez 2001; Martin, Goodwin et al. 2002; Martin 2005; Martin and Kelly 2023). The fauna of GFS includes several Neotominae and Cricetidae incertae sedis that overlap little with that of other contemporaneous sites. Moreover, GFS fauna

consists of some taxa that mainly thrive in Mexico, Central America, and South America today. This diverse and unique assemblage of cricetids underscores the importance of GFS in understanding the origin and evolution of cricetids in the forests of the Appalachian region and broader eastern North America.

CHAPTER 2. MATERIALS AND METHODS

All specimens described in this thesis were recovered from the Gray Fossil Site in Washington County, Tennessee, which dates to the early Pliocene (latest Hemphillian or early Blancan) (Samuels et al. 2018; Samuels and Schap 2021). Cricetid fossils from the site were collected through years of excavation and screen-washing of matrix, using techniques introduced by Hibbard (1949), refined for GFS by Drs. Steven Wallace and Blaine Schubert and Mr. Shawn Haugrud. The wet screen procedure involved the use of 1.7x1.7mm mesh screen boxes to sieve through the silty-clay matrix obtained from various test pits at GFS during field seasons. Identifiable microfossil specimens were recovered by handpicking and sorted under a dissecting microscope. Most micromammal specimens from GFS are isolated cheek teeth, but some intact maxilla and dentary materials with teeth in situ do occur. Some of the teeth and jaw fragments were cleaned and stabilized with Butvar.

Initial identification of some cricetid fossils from GFS was carried out by Dr. Joshua Samuels and Dr. Richard Zakrzewski. The detailed examination presented in this paper was achieved through a qualitative assessment of occlusal morphology and quantitative comparison to modern samples and published fossil records from across North America. All specimens underwent examination under a stereomicroscope and were photographed using a Dinolite AM4815ZT digital microscope camera and Dinocapture 2.0 imaging software. Measurements were taken in ImageJ, an image processing program, capturing the greatest lengths and widths in millimeters with the occlusal surface of each specimen oriented parallel to the photographic plane. The employed dental terminology of occlusal morphology was modified from Kelly and Martin (2022).

58 species of modern and fossil cricetids were studied for qualitative and quantitative comparisons, with specimens of many taxa directly examined and other species derived from literature sources (Appendix A). Taxonomy of cricetids employed here follows Fabre et al. (2012), Kelly and Martin (2022), and Ronez et al. (2021). Dental measurements include the maximum anteroposterior length and maximum mediolateral width of the cheek teeth (first to third molar, Appendix B), as well as crown height of some molars measured from the base of the crown (enamel dentine junction) to the apex of the protoconid (pch). Diversity of fossil cricetids from GFS was compared to the extant cricetids known from Tennessee (Appendix C), as well as cricetids represented at well-known Pliocene fossil sites from across North America. Qualitative characters were scored for each taxon studied (as completeness of specimens permitted), with character states (Appendices D-I) derived from recent studies of cricetids (Kelly and Whistler 2014; Kelly and Martin 2022).

Abbreviations used in the text are: **ap =** anteroposteriorly length, also known as O-L; **GFS =** Gray Fossil Site**; L, R =** locus of the molar within the jaw: left or right; **M# (e.g., M2 =** upper molar (e.g., upper second molar); **m# (e.g., m3) =** lower molar (e.g., lower third molar); **mm** = millimeters; **N =** number of examined specimens; **O-L, O-W =** observed length or width; **pch/ap =** equation used to examine the type of crown height; **pch =** protoconid crown height (measured from the base of the crown (enamel dentine junction) to the apex of the protoconid); **W/L =** ratio of observed width to length.

Institutional abbreviations are as follows: **AMNH**, American Museum of Natural History, New York City, New York; **ETMNH**, East Tennessee State University Museum of Natural History collection, Gray Fossil Site & Museum, Johnson City, Tennessee; **UF**, Florida State

Museum, University of Florida, Gainesville; **USNM**, National Museum of Natural History, Smithsonian Institution, Washington, D.C.

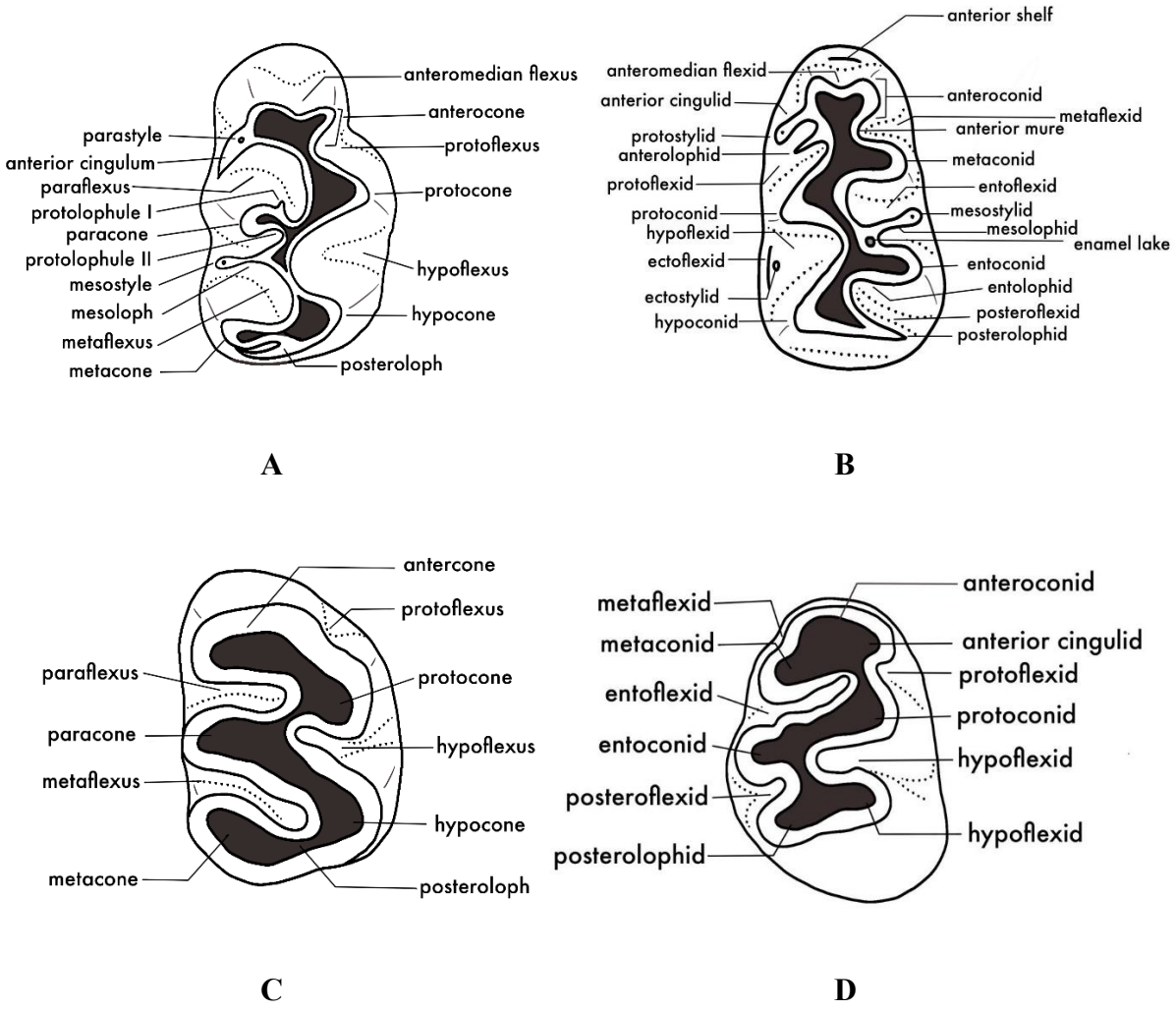

Fig. 1 Dental nomenclature for cricetid teeth employed in this study. Terminology modified from Kelly and Martin (2022). Brachydont tooth: **A**. upper M1, **B**. lower m1. Hypsodont tooth: **C**. upper M1, **D**. lower m1

CHAPTER 3. SYSTEMATIC PALEONTOLOGY

Family CRICETIDAE Fischer de Waldheim, 1817

Subfamily CRICETIDAE incertae sedis Ronez et al. 2021

Genus *POSTCOPEMYS* Lindsay and Czaplewski, 2011

Postcopemys sp. large

(Fig. 2; Table 1; Appendix D&E)

Referred Specimens — ETMNH 8218, 8249, 8250, 8256, 20554, 20834, M1; ETMNH 8202, 16004, 16005, M2; ETMNH 32960, two maxilla fragments, only one with M2 and M3; ETMNH 8235, 13800, 20549, 20551, 20557, m1; ETMNH 8212, 16007, 20549, 20552, 26369, m2.

Description — The maxilla fragment of ETMNH 32960 is missing the part anterior to the posterior alveolus of M1 and the part posterior to M3 (Fig. 2). Only a portion of the palatine is retained. The M2 and M3 are moderately worn and well-preserved.

The M1 from GFS is well-preserved and displays occlusal patterns at varied wear stages. The degrees of wear vary from mild to severe and range in sequence (Fig. 2). ETMNH 20554 is the least worn and has only minor wear on the apices of principal cusps. ETMNH 8250 is heavily worn: all occlusal structures are greatly reduced to the basal crown level. The M1 is brachydont, distinctly large, tapers anteriorly, and is trapezoidal in shape with the labial side being anteroposteriorly longer. The anterior crown wall is inflated, while the posterior is flat and straight. All cusps are bulbous and alternating, with lingual cusps more triangular in shape and posteriorly placed while the labial cusps more conical and anteriorly placed. The protocone is the largest and most inflated cusp of the M1.

The anterocone is situated slightly labial to the midline of the tooth. It is single cusped and transversely expanded in four out of six specimens (Fig. 2). It is pointy anteriorly on ETMNH 8250. The anterocone on ETMNH 20554 is bifurcated by the anteromedian flexi into two subequal-in-size conules, while on ETMNH 8218 it is asymmetrically bilobed with the labial one being slightly larger. The anterocone is always posteriorly linked to the protocone. The parastyle is present on all M1s except ETMNH 8250, and closely positioned to the labial corner of the anterocone and is often attached to the anterocone in four out of six specimens (Appendix D). The parastyle is situated in the middle of the paraflexus on ETMNH 20554 and is well separated from the anterocone and paracone by a narrow but deep groove. The narrow anterior cingulum descends posteriorly from the anterocone towards the protocone. Half of the specimens have a short anterior cingulum that does not reach the protocone nor fully enclose the protoflexus. The posterior arms of the paracone and protocone meet in the center of the tooth. Protolophule I is absent. Almost no alignment of the anterior arm of the hypocone with protolophule II is evident on the M1, only the heavily worn specimen, ETMNH 8250, exhibits a subalignment. The prominent mesoloph usually gets narrower as it descends labially. Two out of six specimens (Appendix D) have a mesoloph that reaches the mesostyle. ETMNH 8249 and 20554 have a flexus ridge that encloses the hypoflexus. A short but wide metalophule is medially connected to the hypocone and can usually be seen on specimens with minute wear (ETMNH 8218, 8256, 20554, 20834). The posteroloph gets narrower as it extends labially to reach the posterior margin of the hypocone. A minute enamel lake is usually present in between the metalophule and the posteroloph. After experiencing more wear, this enamel lake can disappear when the posteroloph merges with the metalophule and broadly connects the metacone and hypocone (Fig. 2B,C).

The M2 is longer than wide and rectangle-in-shape, with an overall occlusal pattern that tapers posterolabially. The anterior crown wall is straight or slightly compressed, showing close contact with the preceding M1. Lingual cusps are triangular in shape, while the labial ones are conical. The principal cusps are symmetrically placed on M2. The opposing cusps tend to become widely confluent with further wear (Fig. 2E). The degrees of wear on M2 vary from mild to severe (Fig. 2D-F). ETMNH 16005 is heavily worn down to the base of the crown with most of the lophs and cusps confluent with one another (Fig. 2E).

The anterocone is absent on M2 and the anterior cingulum is transversely oriented and extends along the anterior crown wall. The prominent labial arm of the anterior cingulum is attached to the anterior crown wall and labially extends without enclosing the paraflexus. The lingual arm of the anterior cingulum is usually indistinct and quickly descends to form a minute shelf at the anterolingual corner of the crown. The relatively narrower lingual arm wraps around the protocone before descending toward the ventrolingual corner of the protocone. A minute protolophule I runs across the paraflexus, linking the protocone anteromedially with the antercone. The more distinct protolophule II connect these two cusps posteromedially. The protolophule I and II become wider with wear and can result in the formation of an enamel lake in between the two cusps (Fig. 2E). A narrow but distinct mesoloph extends from the middle of the median mure toward a minute mesostyle on the labial tooth border. The mesoloph is spur-like and barely reaches the mesostyle, or, in the case of ETMNH 32960 where the mesostyle is absent, does not even reach the tooth border. When it does occur, the mesostyle can appear slightly anteroposteriorly expanded (Fig. 2D-F), anteriorly joining the posterior margin of the paracone and posteriorly to the metacone by a low ridge. The hypoflexus is deep and shelf-like. The posteroloph originates from the hypocone and labially wraps around the metacone.

Specimens with minor wear usually exhibits a feeble mesolophule that joins the posteroloph medially and a posteroloph separated from the posterior margin of the metacone. However, these structures will become confluent with further wear.

The only M3 (ETMNH 32960) is well-preserved and moderately worn like the preceding M2. It has an occlusal triangular pattern with the crown tapered posteriorly. The wear surface is an inverted 'F' shape (Fig. 2F). The anterior crown wall is slightly concave to accommodate the convex posterior wall of the preceding M2. The anterior cingulum is similar to that on M2. The robust labial arm is transversely directed and does not enclose the paraflexus. The lingual arm of the anterior cingulum is greatly reduced but is still recognizable on the anterior crown wall. A more prominent protolophule I medially connects the paracone to protocone and intercepts the paraflexus, creating an anteroposteriorly elongated enamel lake at the midline. The paracone and protocone are posteriorly linked to the metacone and hypocone, respectively. The metacone and hypocone are both small and largely merged with one another, although a small enamel lake is located at the midline to partly separate these two cusps. A minute posteroloph extends from the lingual margin of the hypocone and quickly descends to the ventrolingual corner of the protocone.

The m1 is brachydont, large, and longer than wide. Compared to other m1s from the site, these specimens are more anteroposteriorly compressed (Appendix B). The overall crown tapers anteriorly. The posterior crown wall is usually flat, reflecting the compression from m2. Labial cuspids and lingual cuspids are bulbous and alternate in position. Anteroconid is single-cusped, medially placed, and has an inflated anterior margin. The degrees of wear from mild to severe for these m1s of GFS are in such sequence: ETMNH 20551, 20557, 8235, 13800, and 20549.

ETMNH 20549 is heavily worn down to the basal crown level and many major cuspids and lophids are widely confluent with one another.

The anteroconid is usually placed at the midline and in close proximity to the metaconid. A labial cingulid is usually present to connect these two cuspids, and this connection can be broadened over the course of wear, enclosing the metaflexid to form an enamel lake (ETMNH 8235 and 20557) that can eventually disappear with greater wear. The anteroconid can become widely confluent with the metaconid after being heavily worn (Fig. 2K). However, ETMNH 13800 is an exception: an enamel ridge persists to separate the anteroconid from metaconid even with greater wear. On ETMNH 20551, the metaconid connects to no structure but the anteroconid through a lingually placed lophid. Regardless of the relationship between the anteroconid and metaconid, these cuspids tend to share a smooth lingual margin at various stages of wear, with no or minute remnant of the metaflexid. The prominent anterior cingulid gets narrower as it extends labially. Only on more worn teeth will the anterior cingulid fully encloses the protoflexid (Fig. 2K). The anterior arms of the metaconid and the protoconid independently join the anteroconid near the midline, resulting in a strongly 'L' shaped entoflexid. In one out of the five specimens the metaconid-anteroconid connection is more lingually placed (Fig. 2G). Regardless of how these two cuspids are connected to the anteroconid, it is impossible to build a medial connection between the metaconid and the protoconid at any wear stages (Fig. 2). Accessory cuspids and lophids are uncommon: the mesolophid and the mesostylid are both absent. The orientation of the lophid connections among the cuspids is always anteroposteriorly aligned with the midline, mostly because the posterior arm of protoconid it is short and does not diagonally cross the midline. As such, the entolophid and the posterior arm of the protoconid usually appear to be sub-aligned (Fig. 2G-I). The broad hypoflexid gets wider posteriorly,

encouraging the formation of the flexid shelf. The prominent posterolophid wraps around the entoconid and quickly diminishes before making contact with its posterolingual corner.

The m2 is large, brachydont, and sub-rectangular in outline. The length is only slightly longer than the width (Appendix B, average W/L ratio=0.87). The degrees of wear from mild to severe for these GFS m2s are in the following sequence: ETMNH 16007, 20552, 26369, 8212, 20549. Cuspids on ETMNH 20549 are so greatly reduced that the flexids are elevated while the lophid connections are basined. Both the anterior and posterior crown walls are flat. Major cuspids strongly alternate. The labial cuspids are more triangular in shape, while the lingual ones are more conical.

The distinct anterior cingulid is short and extends labially from the metaconid. The anterior cingulid usually encloses the protoflexid and commonly forms an enamel lake in between itself and the protoconid. Only ETMNH 16007 and 20549 have an anterior cingulid that does not reach the protoconid and fully enclose the protoflexid. The metaconid is anteriorly placed, with its anterior margin being the anterior wall of the crown. The entolophid usually is sub-aligned with the posterior arm of protoconid. Accessory structures like mesostylid and mesolophid are absent. The hypoflexid is usually wide, exposing the shelf-like crown base. The distinctly wide posterolophid directs posterolingually to wrap around and then anteriorly towards the posterolingual corner of the entoconid. Only two out of five specimens (ETMNH 20552, 26369) have posterolophid weakly reaching the entoconid. This structure is hard to observe on ETMNH 20549 as it is obscured by wear.

Remarks — *Postcopemys* sp. large from GFS share many morphological similarities with previously described members of *Postcopemys*. Specimens are not classified into any known species of *Postcopemys*, mainly because their sizes are substantially larger than many modern

and fossil species (Table 1) and many fossil species are known from limited numbers of specimens for comparison.

These mostly isolated M1s and M2s are grouped together based on their distinctly large size, alternation of the robust major cusps, prominent mesoloph and mesostyle (Fig. 2, Appendix D). Being brachydont and lacking complete lophodont structure and accessory rootlets, these specimens are excluded from being assigned to genera like *Antecalomys, Paronychomys,* and *Basirepomys* (Jacobs 1977; Kelly 2013; Kelly and Whistler 2014). GFS specimens show some similarity to taxa often referred to *Copemys*, but there are now no known Pliocene records and many former members have been recently reassigned to *Postcopemys* (Jacobs 1977; Czaplewski 1987, 1990; Lindsay and Czplewski 2011; May 2011; Rincón et al 2016; Ronez et al. 2020), the M1 and M2 from GFS resemble *Postcopemys* in having the following: 1) the non-alignment of the protolophule II and the anterior arm of hypocone; 2) anterocone is very anterolabially placed and results in a trapezoidal shape of M1; 3) the major cusps are more alternated on M1and more opposing on M2; 4) parastyle at the edge of paraflexus on M1; 5) short and narrow anterior cingulum on M1 and M2; 6) protolophule I is absent on M1 but present on M2; 7) strong mesoloph that is sometimes accompanied by a mesostyle; 8) the presence of metalophule and posteroloph that can lead to the formation of enamel lake. The inverted 'F' shape M3 is also almost identical to that of *Postcopemys repenningi* (Lindsay and Czaplewski 2011). The only major morphological difference is that the anterocone is less common to develop bilobed structure on M1 from GFS compared to those from previous record. Size-wise, M1 and M2 are proportionally similar to most *Postcopemys.* They are slightly larger than *Postcopemys repenningi*, overlapping and over the upper range of *Postcopemys maxumensis* and *Postcopemys chapalensis* (Table 1). Specimens from GFS definitely belong to a group of larger *Postcopemys*,

but until more available material is discovered, these specimens are refrained from being assigned to any known species or recognized as a new species.

One issue with grouping these M1 and M2 together is that both types of molars display a similar range of lengths, with M2 being significantly wider (Appendix B). On top of this, it is difficult to obtain any reliable information about the dimension of M1 on ETMNH 32960 due to the incompletely preserved alveoli, and thus challenging to draw direct comparisons between M1 and M2 of *Postcopemys* sp. large. Given the materials available, these M2s are grouped with M1s together under *Postcopemys* sp. large for the time being, but may be assigned to a species with confidence if more complete materials are recovered in the future.

The m1 of *Postcopemys* sp. large from GFS has the following distinct morphological characteristics: 1) a single-lobed anteroconid; 2) complete alternation of major cuspids; 3) closely appressed anteroconid and metaconid that can result in the closure of the metaflexid or merging of two cuspids; 4) no connection between the metaconid and the protoconid; 5) absence of mesolophid and other accessory structures; 6) subalignment of the posterior arm of protoconid and the anterior arm of entoconid that can become more aligned through wear (Appendix E). The complete alternation of the major cuspids, the close positioning of the metaconid and anteroconid, and the frequent development of early lophid/cingulid connection between the metaconid and anteroconid that may later lead to formation of an enamel lake and then the merging of two cuspids resemble these m1s to those of many genera of Cricetidae incertae sedis (*Copemys, Postcopemys*) and of Neotominae (*Lindsaymys*, *Antecalomys*, *Paronychomys*) (James 1963; Lindsay 1972; Jacobs 1977; Lindsay and Czaplewski 2011; May 2011; Kelly 2013; Kelly and Whistler 2014; Rincón et al 2016; Ronez et al. 2020; Ronez et al. 2021; Kelly and Martin 2022).

However, there are distinct morphological and dimensional differences between these m1s and some of the genera mentioned above. The m1 differs from *Copemys* (James 1963; Lindsay 1972; Baskin 1978; Ronez et al. 2020) by having the following: 1) a sub- to distinct alignment of the posterior arm of protoconid and entolophid; 2) lack of strong mesolophid; 3) lack strongly reduced or anteroposteriorly compressed anterolophid; 4) lack of accessory structures. The m1 differs from *Lindsaymys* (Kelly and Whistler 2014, Kelly and Martin 2022) by having the following: 1) low crown height (range of crown height of relatively less worn m1s from GFS: pch/ap = 0.44-0.51; range of crown height of m1 of *Lindsaymys takeuchii* and *Lindsaymys* sp.., cf. *L. takeuchii*: pch/ap = 0.55-0.65); 2) the separation of metalophid and anterior arm of protoconid; 3) lack of short spur from the entoconid; 4) slightly longer and distinctly wider crown dimensions (Appendix E). The m1 differs from *Antecalomys* (Kelly and Whistler 2014) by having the following: 1) rounded and less pointed anteroconid; 2) low crown height (unworn specimens of *Antecalomys coxae*: pch/ap = 0.54-0.55); 3) lack of accessory rootlets (Appendix E).

The m1 resembles *Paronychomys* (Jacobs 1977; Kelly 2013; Kelly and Martin 2022) by the following: 1) alternation of major cuspids; 2) the medially placed subcircular anteroconid appressed to the metaconid; 3) shelf-like flexids, especially hypoflexid; 4) well developed anterior cingulid that connects to the protoconid and encloses the protoflexid; 5) accessory molar stylids and lophids absent. However, the m1 also differs from *Paronychomys* by having the following: 1) relatively low crown height (mean range for *Paronychomys*: pch/ap = 0.53-0.65); 2) lophid connections of the cuspids aligned with the midline; 3) prominent “L” shaped entoflexid that anteriorly extends to separate the metaconid and protoconid; 4) more lingually placed connection between the anteroconid and the metaconid. Additionally, relatively higher-

crowned *Paronychomys* tends to develop stronger lophid connections between the cuspids. That is, the dental fields of the cuspids can easily become widely confluent with the lophids and allowing the alignment of the posterior arm of protoconid and entolophid to become rather strong. These characters, however, are not reflected on the m1 from GFS, as the lophid connections are still incipiently built (Fig. 2; Korth & Delieux 2010).

Several studies had provisionally proposed classifying *Paronychomys* (*Peromyscus*) *antiquus* (Kellogg, 1910) as a member of *Paronychomys* despite a few morphological differences. It has also been suggested to be ancestral to later *Paronychomys* species (Kelly 2013; Kelly and Martin 2022). Despite being much older than GFS, this early Hemphillian species shares several morphological characters with the m1 from GFS. In particular, *Paronychomys antiquus* has a relatively lower crown height (pch-ap = 0.49, Kelly and Martin 2022) than other *Paronychomys*, closely resembling the mean crown height of the m1 from GFS (pch-ap = 0.47). Additionally, the anteroconid of *Paronychomys* is structured similarly to that of GFS specimens, with a lingual connection to the metaconid that can sometimes result in the formation of an internal enamel lake with further wear. However, in contrast to the distinct isolation of the metaconid and protoconid of GFS specimens, these two cuspids of *Paronychomys* are linked before sharing the anterior mure that connects them both to the anteroconid (Fig. 2; Jacobs 1977; Kelly 2013; Kelly and Martin 2022). Given the sparse documentation of *Paronychomys antiquus* and the fact that most *Paronychomys* species only share certain occlusal features, the m1 from GFS is withheld from being assigned to *Paronychomys*.

The m1 resembles *Postcopemys* (Lindsay and Czaplewski 2011; May et al 2011; Kelly and Whistler 2014; Rincón et al 2016) by the following: 1) the anteriorly tapered crown shape; 2)

prominent anterior cingulid; 3) prominent anterior cingulid that terminates on the protoconid; 4) lack of accessory structures other than the mesolophid. Although the m1 from GFS shows an incipient alignment of the posterior arm of protoconid and entolophid, this connection is more prominent on other *Postcopemys*, where the posterior arm of protoconid is considerably longer and more diagonally directed. Additionally, the diagonally directed the posterior arm of protoconid and the alignment are often more distinct on m2 of previously described *Postcopemys* (Lindsay and Czaplewski 2011; May et al 2011; Kelly and Whistler 2014; Rincón et al 2016), but the m2 from GFS consistently displays a sub-alignment of the lophids (Fig. 2J-L). None of the m1 and m2 specimens from GFS has a mesolophid present, which is occasionally displayed, though some are only incipient, on *Postcopemys* (Lindsay and Czaplewski 2011, Rincón et al 2016). On top of these, the m1 also differs from previously described *Postcopemys* by having: 1) less anteriorly placed and pointy anteroconid; 2) lingual connection between the anteroconid and the metaconid; 3) separation of metaconid and protoconid; 4) complete absence of occasionally bilobed anteroconid (Lindsay and Czaplewski 2011; Rincón et al 2016).

The m1 and m2 from GFS are substantially larger than almost all genera mentioned above (Table 1). Although *Postcopemys chapalensis* is about the same size as the ones from GFS and has similar morphology, Ronez et al. (2021) suggested that this taxon may not belong to *Postcopemys*. According to the Character State Analysis (Appendix E) and the comparison table (Table 1) , both m1 and m2 most closely resemble *Postcopemys*, if not considering the style of anterolingual connection between the metaconid and anteroconid.

The lower and upper molars from GFS are allocated to the same *Postcopemys* species primarily based on their large size and morphological similarity to *Postcopemys*. However, unique characteristics (distinct shape of entoflexid, the separation of metaconid and protoconid,

the strong lingual connection of anteroconid and metaconid, and the sub-alignment of the entolophid and the short posterior arm of protoconid) on m1s may suggest these specimens belong to a potentially separate species. Additionally, due to the absence of material that has the associated upper and lower dentition, the current grouping of these molars is merely provisional. It is plausible that the upper and lower molars from GFS, along with those of *Postcopemys chapalensis*, may ultimately be recognized as a new genus distinct from *Postcopemys* (Ronez et al. 2021). However, until more materials are collected, the current taxonomic classification remains the most appropriate generic assignment for the GFS taxon.

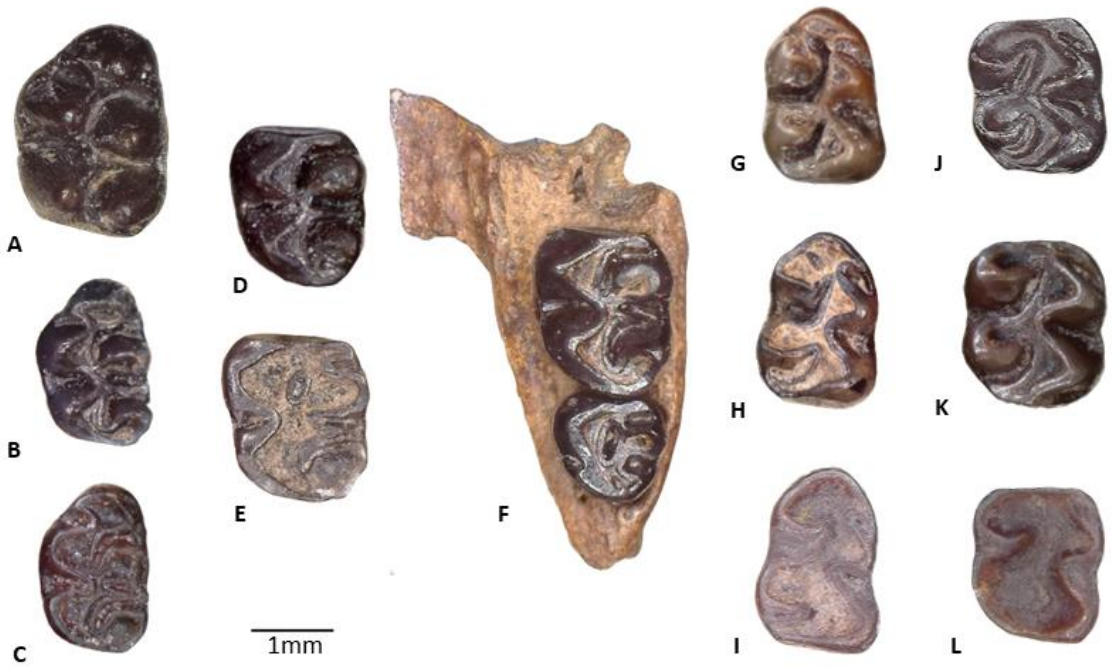

Fig. 2 Upper and lower molars of *Postcopemys* sp. large from GFS. **A**. ETMNH 8218, left M1. **B**. ETMNH 8249, left M1; **C**. ETMNH 8250, left M1; **D**. ETMNH 8202, left M2; **E**. ETMNH 16005, left M2; **F**. ETMNH 32960, right maxilla with M2 and M3 (mirrored for comparison); **G**. ETMNH 20551, left m1 (mirrored for comparison); **H**. ETMNH 8235, right m1; **I**. ETMNH 20549, right m1; **J**. ETMNH 26369, left m2 (mirrored for comparison) ; **K**. ETMNH 20549, right m2; **L**. ETMNH 16007, right m2

Table 1 Measurements (mm) of *Postcopemys* sp. large from GFS and other similar genera. GFS species is highlighted in bold

Species \ Dimension	M1-L	M1-W	M2-L	M2-W	m1-L	m1-W	m2-L	m2-W	reference
***Postcopemys* sp. large**	**1.92-2.47**	**1.3-1.8**	**1.93-2.04**	**1.64-1.8**	**2.03-2.37**	**1.48-1.65**	**1.87-2.04**	**1.59-1.78**	**GFS, this study**
Postcopemys vasquezi†	1.73	1.1-1.13	1.27	1.1	1.27-1.47	0.87-0.97	1.1	0.87	Jacobs 1977
Postcopemys sp., cf. *P. valensis*†	-	-	-	-	1.34-1.38	0.78-0.82	-	-	Kelly & Whistler 2014
Postcopemys valensis†	1.47	0.87	-	-	1.31-1.32	0.78-0.81	-	-	May et al. 2011
Postcopemys sp. *A*†	1.54-1.67	0.93-0.98	1.26	1.1	1.44-1.59	0.9-1.03	1.25-1.31	0.98-1.02	Kelly 2013
Postcopemys sp. *B*†	1.38	0.93	1.05	0.82	1.23-1.31	0.84-0.85	1.03-1.08	0.85-0.96	Kelly 2013
Postcopemys repenningi†	1.72-1.93	1.14-1.41	1.33-1.42	1.12-1.29	1.45-1.54	0.97-1.09	1.38-1.44	1.07-1.11	Lindsay & Czaplewski 2011
Postcopemys maxumensis†	2.02-2.14	1.31-1.34	1.43	1.31	1.85-1.93	1.29-1.31	1.55-1.64	1.38-1.4	Lindsay & Czaplewski 2011
Postcopemys chapalensis†	-	1.83	1.8-1.93	1.63-1.7	2.57	1.4-1.63	1.93-2.17	1.4-1.77	Rincón et al. 2016
Copemys loxodon†	1.80 ± 0.07	1.17 ± 0.07	1.43 ± 0.09	1.29 ± 0.06	-	-	-	-	Ronez et al. 2020
Copemys barstowensis†	2.05-2.06	1.3-1.35	-	-	-	-	-	-	Lindsay 1972
Paronychomys lemredfieldi†	1.68-1.86	0.94-1.09	1.17-1.35	0.95-1.08	1.4-1.73	0.97-1.1	1.17-1.43	0.93-1.13	Jacobs 1977
Paronychomys tuttlei†	1.83-2.17	1.33-1.43	1.5-1.63	1.33-1.37	1.83-1.97	1.17-1.27	1.4-1.83	1.23-1.37	Jacobs 1977
Paronychoms jacobsi†	1.72-1.82	1.13-1.25	1.35-1.46	1.05-1.18	1.51-1.67	0.98-1.08	1.28-1.41	1.03-1.16	Kelly 2013

Postcopemys sp. small

(Fig. 3)

Referred Specimens — ETMNH 14687, 20525, M2; ETMNH 14888, right maxilla fragment with an isolated M2.

Description — ETMNH 20525 is a maxilla fragment with only M2 in situ. The alveolar of M1 is preserved, but the portions anterior to that and posterior to M2 are missing.

The general morphology of *Postcopemys* sp. small is similar to *Postcopemys* sp. large (Fig. 2&3). ETMNH 20525 is heavily worn and major cuspids are widely confluent. ETMNH 14687 and 14888 exhibit a slightly different wear pattern than the one commonly seen on *Peromyscus* sp. large: the shape of wear pattern is triangular on the paracone, unlike the raindrop shape in *Peromyscus* sp. large (Fig. 2D-F, 3B-C). Such development of the wear may allow *Peromyscus* sp. small to exhibit a distinct protolophule I connection in early stage of wear. *Peromyscus* sp. small has a wider and more shelf-like hypoflexus but does not have mesostyle in metaflexus. The more anteromedially oriented metalophule, as seen on ETMNH 14687, allows the formation of an enamel lake bordering the hypocone and metacone.

Remarks — As described above, *Postcopemys* sp. small closely resembles *Postcopemys* sp. large, with only minor morphological differences observed. However, due to the substantial wear evident in two out of three specimens (ETMNH 14888, 20525), it is challenging to identify any additional morphological traits that could potentially further distinguish *Postcopemys* sp. small from *Postcopemys* sp. large. *Postcopemys* sp. small is mainly differentiated from *Postcopemys* sp. large by size: *Postcopemys* sp. small is smaller in overall size, but two out of three molars are proportionally wider than *Postcopemys* sp. large (Appendix B). This lateral expansion of M2

could potentially serve as a diagnostic character for further distinguishing between *Postcopemys* sp. small and sp. large if more materials were present.

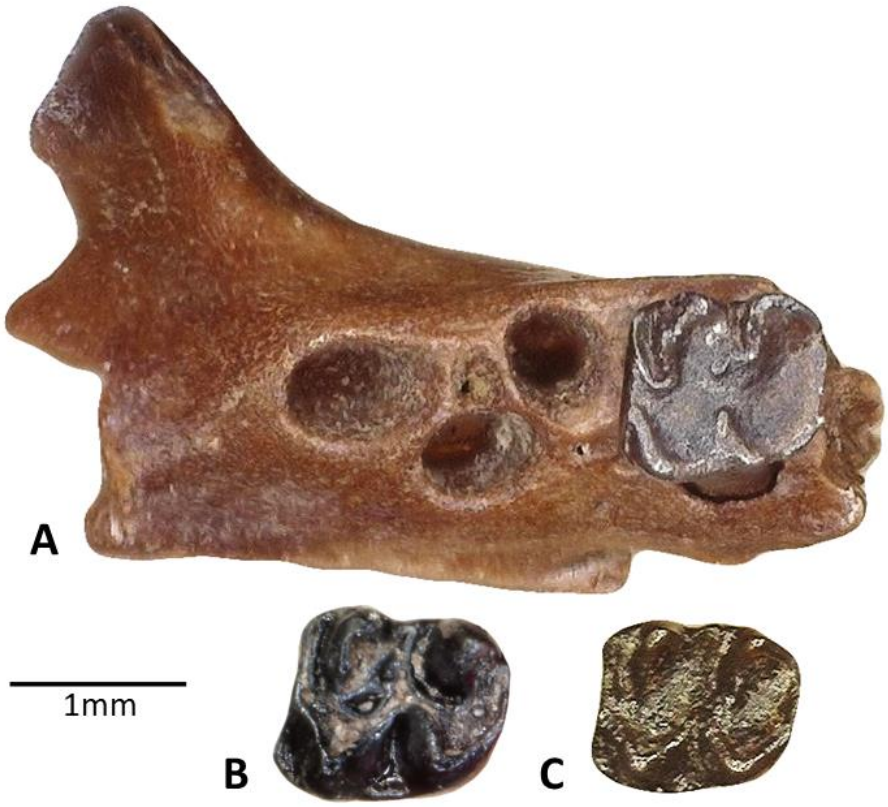

Fig. 3 M2 of *Postcopemys* sp. small from GFS. **A**. ETMNH 20525, right maxilla fragment with M2 (mirrored for comparison for comparison); **B**. ETMNH 14687, left M2; **C**. ETMNH 14888, right M2 (mirrored for comparison for comparison)

Genus *SYMMETRODONTOMYS* Hibbard, 1941

Symmetrodontomys sp.

(Fig. 4; Table 2; Appendix F&G)

Referred Specimens — ETMNH 20555, M1; ETMNH 8245, left dentary fragment with m1-m3; ETMNH 20485, right dentary fragment with m1.

Description — Dentary fragments are preserved in varied conditions (Fig. 4B-E). The material anterior to the mental foramen and posterior to m3 is broken on ETMNH 8245. ETMNH 20485 is missing the portion anterior to the mental foramen, and what succeeds the posterior alveolus of m2. The mental foramen is located anterobasal to the root of m1 and on the dorsal surface of the diastemal ramus, though slightly angled labially, on ETMNH 8245 and 20485. A smooth projecting knob is present at the anterior end of the masseteric crest just below m1, this represents the anterior masseteric crest, which is a fused extension of the masseteric muscle scars (superior and inferior masseteric ridges).

The three-rooted M1 displays moderate premortem wear and is well-preserved (Fig. 4A). It is longer than wide (Appendix B) and the crown tapers anteriorly. A low and indistinct stylar shelf is situated at the base of the anteromedian flexus with a minute anterostyle sitting on the top. The anterocone is slightly asymmetrically bilobed by a deep anteromedian flexus with the labial lobe being slightly larger and taller. The anterocone is posteriorly linked to the protocone by a short anterior mure located lingual to the midline. A blunt parastyle is adjacent to the posterolabial corner of the anterocone. It is located on a descending labial cingulum that connects the anterocone and paracone and encloses the paraflexus. A subtle entoconid is present on the lingual tooth border of the hypoflexus. The thin mesoloph reaches the labial tooth border

while making connection with the posterior margin of the paracone, forming a rounded enamel lake near the midline of the tooth. The presence of the mesostyle is obscured by the wear. No posteroloph is observed, but a posteroloph transversely links the hypocone and the metacone together.

Both specimens have well-preserved m1s that were worn to various degrees that are not severe (Fig. 4B-E). The m1 is longer than wide (Appendix B) and has crown slightly tapers anteriorly. The principal cuspids are largely symmetrically placed with the labial ones being slightly larger and more triangular in shape. The anteroconid is at the midline of the tooth and displays a distinct 'X' shape with an anteromedian flexid bifurcating it into two identical conulids. The short and narrow anterior cingulid extends labially from the anteroconid. It descends posteriorly and terminates before making contact with the protoconid. A protostylid is variably present on the anterior cingulid. The posterior arm of the protoconid is usually aligned with the entolophid. The mesolophid is narrow but always reaching the mesostylid that is weakly present on the lingual tooth border. An incipient ectostylid is present in the hypoflexid of ETMNH 8245. It is very low on the base of the crown shelf and anteroposteriorly elongated. A flexid ridge encloses the hypoflexid of ETMNH 20485. A minute enamel lake is present between the conulids of the anteroconid and the anterior mure. The posterolophid is well separated from the posterior margin of the entoconid and gets narrower as it extends lingually. In ETMNH 20845 the posterolophid is long enough to reach the labial tooth border, but it has a very distinct shape that first directs posteriorly then lingually. Similar structure may have been present in ETMNH 8245 during its early stage of wear.

The m2 is preserved in a similar condition as m1 on ETMNH 8245. It is rectangular in shape and has principal cuspids more symmetrical in position than those on m1 (Fig. 4C). The

short anterior cingulid is labially directed and does not reach the anterolabial corner of the protoconid. The narrow mesolophid is anteriorly directed to reach the lingual tooth corner while being separated from the metaconid. An ectostylid is present on the labial cingulum that wraps around the labial base of hypoconid. The posterolophid directs posteriorly then labially and partially encloses the posteroflexid.

The m3 is well-preserved on ETMNH 8245 (Fig. 4C). It has a flat anterior crown wall, and it tapers posteriorly. The anterior cingulid is very short and descends labially to enclose the protoflexid. The metaconid is more anteriorly placed relative to the protoconid. A short mesolophid is anteriorly reaching the metaconid and partially enclosing the entoflexid. The posterolophid is absent.

Remarks — The dental morphology of the M1 specimen, ETMNH 20555. exhibits several distinctive features. These include slightly alternated cusp positions, presence of a basal shelf and anterostyle anteromedial to the deeply bilobed anterocone, distinct parastyle and mesoloph, and broad flexi. The bilobed anterocone and the sub-symmetrical arrangement of the major cusps are shared traits observed in various brachydont early possible Sigmodontinae genera, such as *Bensonomys*, *Jacobsomys*, and *Symmetrodontomys* (Hibbard 1941; Skinner et al. 1972; Basin 1978; Czaplewski 1987; Martin, Goodwin et al. 2002; Martin, Honey et al. 2002; Lindsay and Czaplewski 2011; May et al. 2011; Kelly and Whistler 2014; Ronez et al. 2021). Although there are individual variations within these genera, *Bensonomys* generally lacks a mesoloph or possesses only an incipient one that does not extend to the border of the tooth (Skinner et al. 1972; Basin 1978; Czaplewski 1987; Martin, Goodwin et al. 2002; Martin, Honey et al. 2002; Kelly and Whistler 2014; Ronez et al. 2021). Additionally, it is uncommon for *Bensonomys* to develop a well-defined labial cingulum at the paraflexus along with a consistent parastyle

(Skinner et al. 1972; Basin 1978; Czaplewski 1987; Martin, Goodwin et al. 2002; Martin, Honey et al. 2002; Kelly and Whistler 2014; Ronez et al. 2021). While it is more often to see *Jacobsomys* develop such structures between anterocone and paracone; the labial cingulum in *Jacobsomys* frequently falls short of reaching the paracone and enclosing the paraflexus (Czaplewski 1987; Lindsay and Czaplewski 2011; May et al. 2011; Ronez et al. 2021). Besides the differences in morphology; *Jacobsomys* generally surpasses ETMNH 20555 in size. With *Jacobsomys dailyi* being the exception to having the same length as ETMNH 20555 (May et al. 2011); it still has greater transverse width (Appendix B). On the other hand, ETMNH 20555 bears a close morphological and dimensional resemblance to *Symmetrodontomys*; as indicated in the Character State Analysis and measurement data presented in the relevant tables (Table 2; Appendix B&F).

The lower molar dental characteristics of specimens from GFS exhibit remarkable similarities with those of previously described *Symmetrodontomys* (Martin, Goodwin et al. 2002; Martin, Honey et al. 2002; Ronez et al. 2021). Notably, these similarities include the following: a distinct knob-like anterior masseteric crest that ends just beneath the anterior root of m1 (Hibbard 1941; Dalquest 1978; Martin, Goodwin et al. 2002; Zijlstra et al. 2014); the dorsal placement of the mental foramen on the diastemal ramus; a slightly tapered anterior crown; a pattern of slightly alternating opposing cuspids with a mostly confluent dental field on m1; transitioning to a more opposing configuration on m2 and m3; a prominently bifurcated anteroconid with two equal-sized and symmetrically placed conulids; forming an ‘X’ pattern between anteroconid; protoconid and metaconid (Martin, Goodwin et al. 2002; Martin, Honey et al. 2002). Moreover, the overall size of the GFS specimens falls within the range of known *Symmetrodontomys* (Hibbard 1941; Martin, Goodwin et al. 2002; Martin, Honey et al. 2002).

However, it is important to note a distinct difference between GFS specimens and other described *Symmetrodontomys*: the GFS specimen exhibit fewer accessory structures, such as the stylids in the labial flexids.

While the lower molars from the GFS site also share some morphological characters with other sigmodontines (Appendix G), their overall crown size, the positions of the cuspids, and the frequency of accessory stylids and lophids distinguish them from several genera. For instance, *Jacobsomys* and *Bensonomys* occasionally display a transversely elongated and asymmetrically positioned labial conulid of anteroconid, which can result in a more labially tapered anterior crown in certain specimens (e.g., Czaplewski 1987; Ronez et al. 2021). Additionally, the anterior mure can be longer in some *Jacobsomys* and *Bensonomys*, precluding the formation of "x" pattern between anteroconid, protoconid, and metaconid (Martin, Goodwin et al. 2002; Martin, Honey et al. 2002). The mesolophid also is less common in *Bensonomys* (Skinner et al. 1972; Basin 1978; Czaplewski 1987; Martin, Goodwin et al. 2002; Martin, Honey et al. 2002; Kelly and Whistler 2014; Ronez et al. 2021). When comparing size, GFS specimens are on the larger end of the size range of *Bensonomys*. They are similar to *Bensonomys* sp., but could proportionally be wider (Table 2). When compared to *Jacobsomys*, however, GFS specimens appear smaller.

In summary, it is most appropriate to assign GFS specimens to the genus *Symmetrodontomys*. Relative to *Symmetrodontomys simplicidens*, GFS specimens closely resemble *Symmetrodontomys dammsi* (Martin, Goodwin et al. 2002) based on their morphological characteristics and size (Table 2; Appendix F&G), but additional specimens would help provide more confidence in a precise taxonomic assignment. Until more specimens are recovered, the GFS specimens are designated as *Symmetrodontomys* sp.

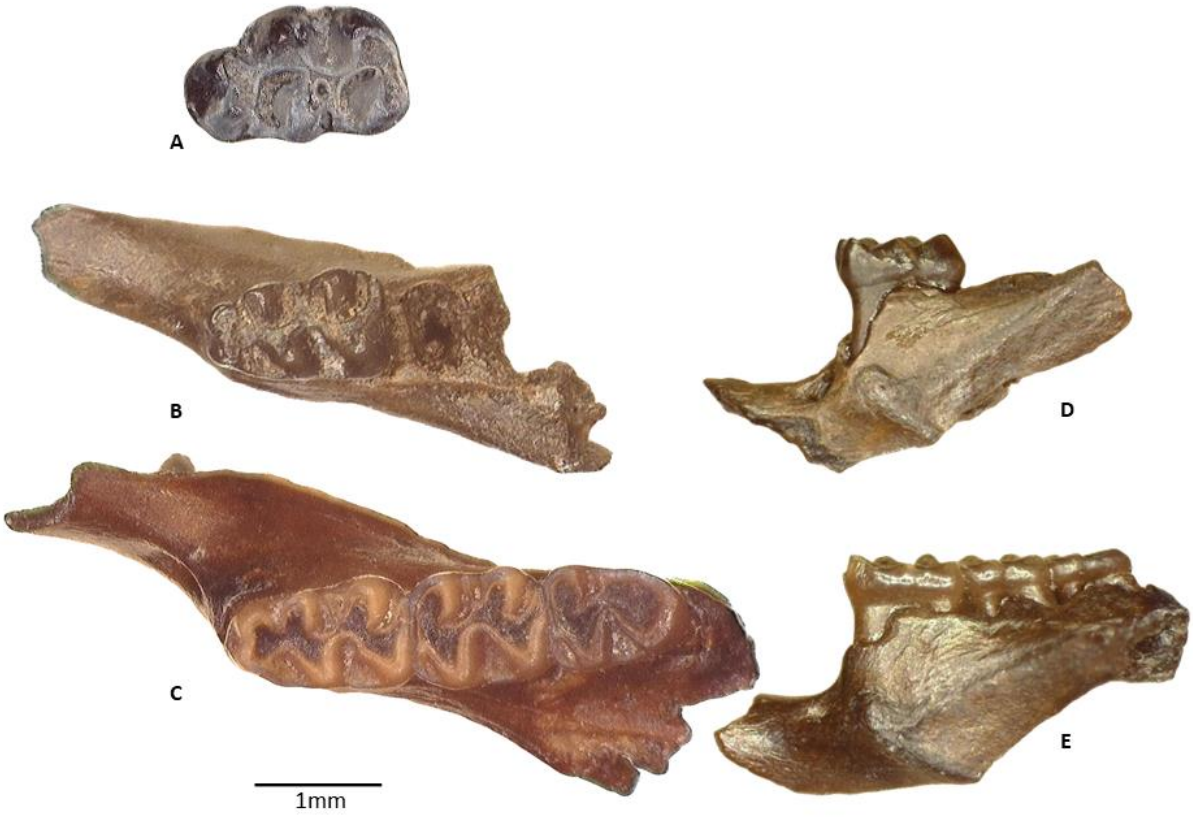

Fig. 4 Upper M1 and dentary fragments of *Symmetrodontomys* sp. from GFS. **A**-**C**: in occlusal view. **D**-**E**: in labial view (not scaled). **A**. ETMNH 20555, right M1; **B&D.** ETMNH 20485, right dentary with m1 (mirrored for comparison); **C&E**. ETMNH 8245, left dentary with m1 to m3

Table 2 Measurements (mm) of *Symmetrodontomys* sp. from GFS and other similar genera. GFS species is highlighted in bold

Dimension / Species	M1-L	M1-W	m1-L	m1-W	m2-L	m2-W	m3-L	m3-W	reference
***Symmetrodontomys* sp.**	**1.7**	**1.13**	**1.45-1.53**	**0.91-0.95**	**1.12**	**0.85**	**1.13**	**0.83**	**GFS, this study**
Symmetrodontomys daamsi†	1.6-1.94	1.03-1.23	1.38-1.83	0.9-1.18	1.11-1.42	0.99-1.2	1.01-1.45	0.95-1.03	Martin, Goodwin et al. 2002
Symmetrodontomys simplicidens†	1.73-1.95	1.08-1.26	1.75-1.8	1.11-1.13	1.3-1.37	1.05-1.13	1.06-1.26	0.94-0.99	Hibbard 1941; Martin, Honey et al. 2002
Jacobsomys verdensis†	2.26	1.47	2.06	1.31	-	-	-	-	Czaplewski 1987
Jacobsomys dailyi sp. nov. †	1.83-1.91	1.32	1.56-1.68	0.98-1.1	1.17-1.24	1.05-1.14	1.23-1.27	0.93-0.98	Lindsay & Czaplewski 2011
Jacobsomys dailyi†	1.7	1.18-1.23	1..69-1.82	1.06-1.08	1.36-1.4	1.11-1.18	1.25-1.33	0.98-1.03	May et al. 2011
Bensonomys sp. †	1.7-1.72	1.1-1.13	1.64-1.65	1.07-1.08	1.25-1.26	1.05-1.1	1.04	0.82	Kelly and Whistler 2014
Bensonomys gidleyi†	1.58-1.7	1.05-1.13	1.35-1.48	0.88-0.98	1.03-1.17	0.95-1.1	0.93-1.05	0.75-0.9	Baskin 1978
Bensonomys yazhi†	1.37-1.47	0.9-0.97	1.2-1.37	0.75-0.9	0.9-1.05	0.85-0.97	0.75-0.83	0.6-0.75	Baskin 1978
Bensonomys arizonae†	1.61-1.69	1.08-1.18	1.51-1.71	1.06-1.16	1.13-1.21	1.03-1.15	1.04-1.05	0.9-0.92	Czaplewski 1987
Bensonomys meadensis†	1.62-1.65	0.99-1.02	1.55-1.6	0.95-1.02	1.23-1.24	0.98-1.09	-	-	Martin, Honey et al. 2002

Subfamily SIGMODONTINAE Wagner, 1843

Tribe Oryzomyini Vorontsov, 1959

(Fig. 5; Appendix H)

Referred Specimens — ETMNH 32961, right dentary fragment with m1-m3.

Description — Only the horizontal ramus supporting the tooth row remains on ETMNH 32961, the specimen is broken just anterior to m1 and posterior to m3 (Fig. 5). There is no knob present at the anterior end of the masseteric crest. Brachydont m1 to m3 are well preserved and only experienced moderate wear. Double-rooted molars have slightly offset cuspids and anteroposteriorly wide flexids that contribute to the distinct length of the teeth.

The m1 of ETMNH 32961 has an anteriorly tapered and convex crown with somewhat triangular cuspids (protoconid, metaconid, hypoconid, entoconid) (Fig. 5). There is no anteromedian flexus present to separate the anteroconid, since the anterior wall of the crown is completely convex and show no sign of groove. The anteroconid is symmetrically placed and has an anterolabial cingulid that extends posteriorly and descends until reaching the protoconid. The lingual cuspids are slightly anteriorly placed, allowing the metaconid to be largely confluent with the anteroconid. However, a shallow metaflexid separates the anteroconid and metaconid lingually. The protoconid and metaconid share a wide connection to the anteroconid. The posterior arm of protoconid is aligned with the anterior arm of entoconid. The anterior and posterior mures are aligned with the midline of the tooth. The remains of a transversely elongated mesostylid (or a short mesolophid) lies just anterior to the entoconid, but its presence is obscured by the wear. The ectolophid appears to be incipient, possibly due to wear, and it reaches the labial border of the tooth. The ectostylid is absent. The posterolophid extends from

the hypoconid posterolingually to wrap around the entoconid, while being mostly separated by a posteroflexid until terminating on posterolingual margin of entoconid.

The m2 of ETMNH 32961 has a rectangular shape and is longer than wide (Fig. 5; Appendix B). The anterior cingulid is either minute and lost to wear or absent. The labial cuspids are slightly larger and more triangular in shape than the lingual ones. The meta-protoconid and ento-hypoconid pairs each share a widely transverse dental field. The anterior and posterior mures connecting these dental fields are aligned with the midline of the tooth. The entoflexid and hypoflexid are distinctly wide and expose the shelf-like crown base. An incipient mesostylid is connected by the mesolophid. A minute ectostylid is present in the hypoflexid and is linked to a weak and narrow basal cingulid that wraps around the hypoconid and ends on its posterior margin. The posterolophid is first posteriorly directed then extends lingually without reaching the entoconid, leaving the posteroflexid open at the border of the tooth.

The m3 of ETMNH 32961 has an overall dumbbell shape and its crown tapers posteriorly (Fig. 5). The anterior cingulid is narrow and quickly descends labially. The transverse dental fields shared by the cuspids (meta-protoconid and ento-hypoconid pairs) are linked by a long median mure. The entoconid and hypoconid are placed close to one another and greatly confluent. The posterolophid is short but distinguishable from entoconid due to the presence of a weak posteroflexid. A very narrow basal ridge extends off the lingual side of the entoconid, wraps around the posterior wall of the crown and the hypoconid, then stretches anteriorly to enclose the hypoflexid.

Remarks — ETMNH 32961 exhibits distinctive dental characteristics (Appendix H), including a single-lobed anteroconid, a symmetrical arrangement of major cuspids, transversely oriented flexids, a linear alignment of the anterior and median mures along the midline of the tooth, lack

of accessory structures, and a distinct dumbbell shape of m3. The symmetrical placement of major cuspids is more distinct in m2 and m3. This cuspid arrangement places ETMNH 32961 in Sigmodontinae and it bears a resemblance to Oryzomyini when considering other morphological characters.

Oryzomyini such as *Oryzomys* and *Oligoryzomys* commonly develop strongly opposing cuspids, where the anterior margins of opposing cuspids align transversely (Hershkovitz 1971; Voss et al. 2002; Weksler 2006; Turvery et al. 2010; Ronez et al. 2023). Instead of the anteroposterior alignment of the anterior and posterior mures along the midline, these genera also tend to feature more diagonally oriented mures that form a zigzag loph pattern in occlusal view. The proximity of anterior and posterior cuspids correlates with the degree of diagonal orientation in these mures and the narrowness of the flexids. This compact cuspid arrangement contributes to the reduction of the anteroposterior crown length, which typically relates to a transversely directed posterolophid rather than a posterior one. In contrast, ETMNH 32961 displays a spacious arrangement of cuspids and lophids more akin to *Zygodontomys*. This resemblance extends to the presence of a single-lobed anteroconid, a posteriorly widening hypoflexid, a widely opened posteroflexid, and an initially posteriorly directed posterolophid (Voss 1991; Solorzano et al. 2015; Ronez et al. 2023). Furthermore, ETMNH 32961 shares a similar size with *Zygodontomys brevicauda* as reported by Solorzano et al. (2015) in terms of molar dimensions (*Zygodontomys brevicauda*: m1-L=1.9, m1-W=1.2, m2-L=1.5, m2-W=1.2, m3-L=1.4, m3-W=1.0; Solorzano et al. 2015). However, the size of the molar may not be a diagnostic trait that can aid in making the final assignment of ETMNH 32961.

The primary distinction between *Zygodontomys* and ETMNH 32961 lies primarily in the orientation of the cuspids. *Zygodontomys* typically exhibits a posterior pair of transverse cuspids

angled posteromedially. ETMNH 32961, however, features the posterior pair of these cuspids angled anteromedially (Fig. 5). Moreover, *Zygodontomys* tends to have flexids free of accessory structures, while there are still some weak presences of stylids and lophids on ETMNH 32961. There is also a slight difference in the crown height of *Zygodontomys* and ETMNH 32961, with GFS specimen being more brachydont. Nevertheless, this may not be a diagnostic character since most of the comparable records of *Zygodontomys* are from the late Pleistocene and many cricetids have a tendency to develop higher crowned crown over time. The limited availability of comprehensive *Zygodontomys* records and specimens similar to ETMNH 32961 from GFS poses a challenge in confidently identifying this specimen at the genus level based solely on a single tooth row.

Fig. 5 The right dentary of Oryzomyini (ETMNH 32961) from GFS. In occlusal view

Subfamily NEOTOMINAE Merriam, 1894

Tribe PEROMYSCINI Cockerell and Printz, 1914

Genus *PEROMYSCUS* Gloger, 1841

Peromyscus sp.

(Fig. 6; Table 3; Appendix I)

Referred Specimens — ETMNH 20548, m1; ETMNH 8252, m3; ETMNH 20558, left dentary fragment with m3; ETMNH 12288 and 20838, left dentary fragment with m1 and m2; ETMNH 36765, right dentary fragment with m2 and m3; ETMNH 8247, left dentary fragment with m1-m3.

Description — The dentary materials are incomplete. On ETMNH 12288, only the portions behind the diastema and partial ramus are preserved. The incisor structure, ventrodistal portion of the dentary, m3, and the dorsal portion of the ascending ramus are lost. This material may have experienced some postmortem wear on the dorsal surface of the ramus as it appears smooth. There is one minute and oval foramen present in the masseteric fossa. Another hole situated distal to that oval one has an irregular outline. The edge of this hole is sharp and fresh, suggesting it to be the result of postmortem impacts on the dentary. A distinctly robust ridge is horizontally oriented on the ramus. On ETMNH 20838, only the diastemal ramus and the anterior part of the ramus are preserved. The anterior root of m3 is left inside of the alveolus. The incisor structure and the material posterior to the half of the distal alveolus of m3 are missing. The anterior alveolus of m1 is lost on the remaining dental fragment, leaving the anterior root of m1 exposed. The dentary of ETMNH 36765 is highly concreted with only m2, m3, and portion of the ramus between the coronoid process and the condylar process preserved and exposed. The

tip of the coronoid process is eroded and missing. A postmortem foramen is present on the medial side of the remaining portion of the dentary, exposing the incisor canal. The dentary of ETMNH 8247 preserves the posterior half of the diastemal ramus and the ramus supporting the entire tooth row.

The mental foramen on these dentary fragments is usually anteroventral to the root of m1 and on the horizontal-dorsal surface of diastemal ramus, while the opening slightly angled labially. The anterior margin of the masseteric crest starts posterior to the mental foramen on ETMNH 12888 and ventroposterior on ETMNH 8247 and 20838 (Fig. 6; Appendix I). The ridges of the masseteric crest are more robust on ETMNH 8247 and 20838. The roots of the tooth row are exposed as the tooth rows are usually elevated (Fig. 6).

The m1 is sub-rectangular in shape and is longer than wide (Appendix B). The m1 has a distinct tapered anterior crown and a transversely straight posterior crown wall. The major cusps are usually alternatively placed, except on ETMNH 12288 the cuspids on opposing sides are broadly confluent and show more of a symmetrical pattern. The lingual row of the cusps are situated more anteriorly. The degrees of wear on the m1 vary from mild to severe (Fig. 6). ETMNH 20548 is distinctly less worn and better preserved than others. The anteroconid is single-cusped, anteriorly inflated, and placed at the midline of the tooth. The spur-like anterior cingulid usually shares an anterior wall with the anteroconid as it extends toward the protoconid. It is well separated from the protoconid until it reaches the ventrolabial corner of the protoconid and enclose the protoflexid. However, the separation of the anterior cingulid and protoconid is usually obscured by the wear on m1s other than ETMNH 20548. ETMNH 20838 was so heavily worn that the anteroconid and anterior cingulid are largely confluent with the metaconid and protoconid. The metaconid and the protoconid meet at the midline and collectively join the

posterior anteroconid through the anterolophid. The protoconid is widely confluent with the metaconid. The alignment of the posterior arm of protoconid and the entolophulid is present in three out of four specimens, except ETMNH 12288. The relatively opposingly placed cuspids and the relatively long median mure make such the alignment impossible. The mesolophid variedly present. On ETMNH 20548, the mesolophid is short but wide, and it reaches the lingual tooth border. The mesolophid on ETMNH 20838 is widely confluent with the anterior portion of the entoconid. It is separated from the posterior margin of the metaconid by a small enamel lake, but the lingual end of the mesolophid directs anteriorly and connects with the metaconid at its posterolingual corner. ETMNH 12288 may not have a mesolophid, but a very short and subtle mesostylid that is medially placed in the entoflexid. The hypoflexid is wide and shelf-like. A distinct indentation, possibly the result of postmortem breakage, is present on the enamel edge of the entoconid of ETMNH 12288 and the entoconid and hypoconid of EMTNH 20838. The indentation on the entoconid is deeper and more distinguishable. The posterior cingulid extends from the hypoconid and wraps around the entoconid, while being well separated from it, to reach the lingual tooth border.

All m2s are situated in fragmented dentaries. The degrees of wear on these m2s is similar to the associated m1s. The m2 is rectangular in shape and is longer than wide. Most of the structures are greatly reduced and merged with one another, except the one of ETMNH 36765 showing only moderate wear. The anterior cingulid is usually short but distinct and encloses the protoflexid: it extends labially and terminates at the anterolabial margin of the protoconid. The heavy wear can contribute a wide but very short posterior mure that connects all the principal cusps while entoflexid and posteroflexid greatly reduced or disappeared. The posterior arm of protoconid is aligned with the entolophid, even on ETMNH 12288. However, this alignment

could be a biased result of the wear. The occurrence of mesolophid varies. The mesolophid of ETMNH 20838 is reduced and can only be recognized by a short spur-like structure posterior to the metaconid. The mesolophid of ETMNH 12288 and 8247 is weakly present and largely confluent with the entoconid. There is no mesolophid on ETMNH 36765. The distinctly wide hypoflexid is the best-preserved flexid on m2 at all wear stages. A wide posterior cingulid extends lingually from the hypoconid and is usually attached to the posterior margin of the entoconid. The posterior cingulid of ETMNH 12288 is fully merged with the entoconid and the hypoconid as the posterior margin of the entoconid gets wore away.

The crown of m3 distinctly tapers posteriorly, has a general S shape occlusal pattern, and the principal cuspids are largely merged with one another with greater wear. The metaconid is slightly anterior to the protoconid. Cuspids posterior to these two cuspids are merged into one structure and shares the posterior crown wall. All cuspids are connected by a continuous lophid. The lingual entoflexid of ETMNH 36765 is enclosed by a robust enamel ridge, forming a transversely directed enamel lake. Such a structure is not clear to see on ETMNH 8247 due to the wear. The hypoflexid is enclosed by a subtle and low ridge on the tooth border.

Remarks — *Peromyscus* is recognized for its alignment of protolophule II and the anterior arm of the hypocone on the upper molars, as well as the posterior arm of the protoconid and the entolophid on the lower molars (Lindsay and Czaplewski 2011). This alignment is evident in almost all specimens from GFS, with the exception of ETMNH 12288. Additionally, these specimens also exhibit cusp(id)s alternation and long and diagonally directed lophid connection. Specimens from GFS also share several similarities with *Peromyscus*, including: 1) an elongated crown that tapers anteriorly on m1; 2) a prominent posteroloph(id); 3) a lack of accessory rootlets; 4) narrow flexi and flexids.

Peromyscus sp. from GFS falls on the smaller end of the *Peromyscus* size spectrum and closely resembles the contemporaneous *Peromyscus hagermanensis* in terms of size (Table 3). The specimens from GFS resemble *Peromyscus hagermanensis* in the following features: 1) a more developed alignment on lower molars after wear; 2) a broad posteroloph(id) that reaches the posterior corner of the entoconid and partially encloses the posteroflexid on m1 and m2; 3) varied presence of a short mesolophid and mesostylid. However, they also differ from *Peromyscus hagermanensis* (Tomida 1985; Ruez 2001) in several aspects: 1) a bilobed anteroconid on m1 is less developed; 2) accessory structures (e.g., the parastyle, ectostylid/lophid, and flexus ridges) on both upper and lower molars are less frequently observed (Hibbard 1962, Tomida 1985). *Peromyscus* sp. also differs from other *Peromyscus* (e.g., *P. sarmocophinus, P. maximus*, *P. complexus*) mainly in the lack of different accessory structures in the flexi and flexids (e.g., ectostylid, ectolophid, parastyle), only the mesoloph(id) is consistently observed on *Peromyscus* sp. from GFS (Appendix I).

In essence, *Peromyscus* sp. seldom develops prominent accessory structures and tends to have simple and open flexi(ds). *P. hagermanensis* is considered the earliest *Peromyscus* (Kelly and Martin 2023) and first appeared in the early Pliocene (between 4.98 and 4.90 Ma, Panaca NV; Mou 2011). Given the inferred age of the site, *Peromyscus* sp. from GFS could be evidence of their early expansion across North America or it could possibly represent the earliest record of the genus.

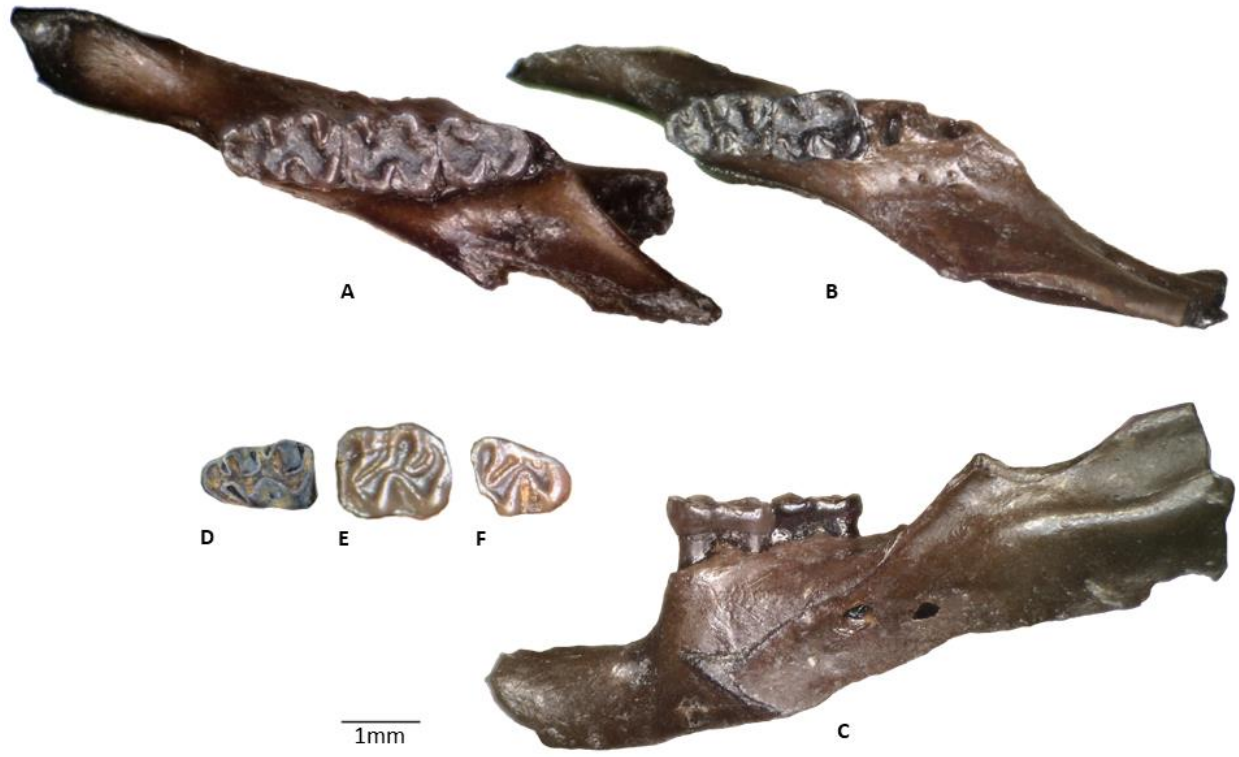

Fig. 6 Dentary and lower molars of *Peromyscus* sp. from GFS. **A**,**B**, **D**, **E**, **F**: in occlusal view. **C**: in lateral view. **A**. ETMNH 8247, left dentary with m1 to m3; **B**-**C**. ETMNH 12288, left dentary with m1 and m2; **D**. ETMNH 20548, left m1; **E**-**F**. ETMNH 36765, right dentary with **E**. m2 and **F**. m3

Table 3 Measurements (mm) of *Peromyscus* sp. from GFS and other extinct and extant taxa. GFS species is highlighted in bold

Species \ Dimension	m1-L	m1-W	m2-L	m2-W	m3-L	m3-W	reference
***Peromyscus* sp.**	**1.38-1.57**	**0.86-1.01**	**1.08-1.46**	**0.89-1.21**	**1.02-1.28**	**0.81-1.02**	**GFS, this study**
Peromyscus hagermanensis†	1.46-1.7	0.94-1.06	1.16-1.34	0.96-1.08	0.941.14	0.76-0.86	Tomida 1985
Peromyscus sp. cf. *P. hagermanensis*†	1.64-1.68	1.05-1.19	1.3-1.52	0.95-1.12	-	-	Albright 1999
Peromyscus sp. cf. *P. baumgartneri*†	-	-	-	-	-	-	Albright 1999
Peromyscus maximus†	-	-	-	-	-	-	Albright 1999
Peromyscus leucopus	1.28-1.63	0.79-1.03	1.06-1.26	0.85-1.11	-	-	ETMNH collection USNM collection
Peromyscus maniculatus	1.2-1.6	0.85-1.02	1.08-1.37	0.85-1.1	-	-	Lindsay 1972 ETMNH collection
Peromyscus truei	1.55-1.8	1-1.2	1.2-1.5	1-1.25	-	-	Lindsay 1972
Peromyscus	1.56-1.68	0.93-1.01	1.36	1.02	1.03	0.94	UF collection

Genus *NEOTOMODON* Merriam, 1898

Neotomodon sp.

(Fig. 7&8, Table 4)

Referred Specimens — ETMNH 788, left maxilla fragment with M1; ETMNH 25893, m1; ETMNH 8242, left dentary fragment with m1 and m2; ETMNH 16013, right dentary fragment with m1 and an isolated incisor.

Description — Two fragmentary dentaries have been recovered from GFS, ETMNH 8242 and 16013. The dentary fragment of ETMNH 16013 only preserves m1 and a partial alveolus of m2. Part of the diastema, about 1.5 mm anterior to the mental foramen, is broken and missing, along with most of the posterior ramus. The mandibular canal is exposed in lingual view. This dentary fragment experienced considerable postmortem wear, particularly along the anterior tip of masseteric ridge and the broken edge of the remaining diastema. The mental foramen is situated on the labial surface of the dentary, located 0.5mm anterior and 1.2mm ventral to the root of m1. The tooth row does not appear elevated, rather, the diastema is at about the same level to the crown base of the tooth. The posterior part of diastema, m1, m2, and most of the alveolus of m3 are preserved in ETMNH 8242. The mental foramen is in the middle of the diastema and angles slightly dorsolabially. The dorsal masseteric ridge is partly preserved and is protruding on the labial side of the dentary (Fig. 7). The tooth row is relatively elevated compared to that of ETMNH 16013.

The M1 (Fig. 7D) is worn down to the base but well-preserved postmortem. It is mesodont and has an occlusal ‘M’pattern with no accessory structures present. The anterior crown wall is rounded while the posterior one is vertical. A distinct protoflexus is present on the

anterolingual corner of the crown and separates the anterocone and protocone. The loph connections between cusps are broad but not so widely confluent that the cusps are obliquely aligned. Thus, the angles of the lingual and labial flexi are notably alternated.

The m1 display planned occlusal patterns and show incipient coronal hypsodonty, as the flexids do not extend all the way to the crown base (Fig. 7E,F). Two out of three specimens experienced moderately worn but are well-preserved. ETMNH 8242 is less worn but is missing the entoconid and labial portion of the posterolophid. ETMNH 25983 is smaller but has a similar W/L ratio to ETMNH 16013 (Appendix B). ETMNH 8242 has a proportionally narrower crown, compared to the other two m1s (Fig. 7). Both ETMNH 25983 and 16013 have crowns slightly narrow anteriorly . The anteroconid is enlarged and anteriorly placed on the midline. Only one specimen (ETMNH 16013) features a symmetrically bilobed anteroconid. The anteroconid is posterolingually linked to the metaconid and posterolabially linked to the protoconid. On ETMNH 8242, however, the anterior mure is present on anteroconid to posteriorly connect to the anterior arms of both metaconid and protoconid. The presence of this anterior mure allows ETMNH 8242 to have a more distinct and longer metaflexid and protoflexid. The other two specimens, on the other hand, feature a much shallower and groove-like metaflexid, which only slightly differentiates the metaconid and anteroconid. A shallow and oval shape enamel lake may be present in the anteroconid of ETMNH 8242. A reduced anterior cingulid extends labially and does not reach the protoconid. However, the anterior cingulid on ETMNH 8242 is distinctly longer and posteriorly directed, resulting in a more anteriorly extended protoflexid, as well as a more posteriorly placed protoconid. The protoconid and entoconid are confluent and aligned obliquely, with a subtle projection, possibly the metalophid, near the anterior margin of the entoconid (ETMNH 16013, 25983). Judging from the remaining protoconid, ETMNH 8242 may

not have a as confluent protoconid-entoconid pair as that on the other two specimens The connection between the posterior arm of the entoconid and the hypoconid is more lingually placed, and thus more obliquely directed, on ETMNH 16013 than on EMTNH 25983. The posterolophid is wider on ETMNH 25983 and does not reduce as it extends lingually. A distinct projection is present on the anterior margin of the hypoconid in ETMNH 8242, while it is very incipient in ETMNH 25983 and almost imperceptible in ETMNH 16013. ETMNH 8242 exhibits a small posterior indentation between the hypoconid and the posterolophid. In essence, the lophids are more obliquely directed and the flexids are parallel to one another on ETMNH 8242 and 25983, compared to those on ETMNH 16013. The entoflexid extends more anteriorly in ETMNH 16013, but more labially and even pass the midline of the tooth in ETMNH 25983. As a result, there is a wider confluence of the metaconid and anteroconid in ETMNH 25983.

The m2 in ETMNH 8242 is missing the anterolingual portion of the anteroconid (Fig. 7B). The protoflexid is short but distinctly present, opposing the entoflexid. The anterior cingulid exhibits an incipient labial connection with the protoconid. The entoflexid has an oblique connection with the hypoconid. A small anterior projection, possibly mesolophid, is present on the anterolingual margin of the hypoconid. The posterolophid extending from the hypoconid curves anteriorly at its lingual end. A small indentation on the posterior wall of the tooth is present at the junction of the hypoconid and the posterolophid. The hypoflexid is the deepest and widest flexid that alternates with the posteroflexid.

Remarks — *Neotomodon* has not previously been reported from the fossil record of North America, with the exception of the late Pleistocene occurrences from Mexico (Alvarez 1966; Cruz-Muñoz et al. 2009; Ferrusquía-Villafranca et al. 2010). In comparison to the size of modern *Neotomodon*, the specimens from GFS are smaller than general *Neotomodon alstoni*. They are

slightly shorter than *Neotomodon alstoni perotensis* from the USNM collection, but potentially wider in proportion (Table 4).

All GFS specimens demonstrate robust loph connections without being truly hypsodont: they display an incipient hypsodont pattern, characterized by relatively shallow flexi(-d)s that do not extend to the crown base (Fig. 7). This feature may also reflect the close relationship of *Neotomodon* with *Peromyscus* (as evidenced by molecular studies), which exhibits brachydont dentition. The molars from GFS resemble extant *Neotomodon* (Merriam 1898; Hoffmeister 1945; Korth 2011) in having the following: 1) higher crowned molars; 2) anteromedially placed anterocone (id); 3) many projections from the major cusp(id)s; 4) labial projection on the hypoconid that is common on m1 and to a lesser extent on m2; 5) loph(id)s not strongly confluent with the cusp(id)s obliquely and thus do not have distinctly opposite flexi(ds); 6) prominent posterolophid that is separate from entoconid until further wear; 7) broad lophids are easy to develop, and cusps lose their individuality with slight wear; 8) distinct protoflexus on M1. The assignment of the M1 from GFS to *Neotomodon* not *Neotoma* is mainly based on the direction of the flexi, the alignment of the cusps, and the diminutive size. The widely confluent lophs between the cusps, the notably obliquely aligned cusps, and the obliquely opposite flexi are the advanced traits of some truly hypsodont and lophodont taxa like *Neotoma* (Martin and Zakrzewski 2019), that may not fully develop on specimens of *Neotomodon* sp. from GFS.

The occlusal pattern of both fossil and modern *Neotomodon* exhibits notable variation at different stages of wear, especially on lower molars (Fig. 7&8). Among the specimens studied, ETMNH 8242 is the least worn, retaining many accessory projections and flexids that tend to disappear with wear. For example, the metaflexid is clearly discernible on ETMNH 8242, while it has reduced to a mere groove on the anterior crown of the tooth on ETMNH 16013 and 25983.

Furthermore, there is observed variability in morphology among individuals. In the modern collection of *Neotomodon* from AMNH and USNM, the relationship between the anteroconid, metaconid, and protoconid displays substantial diversity, likely due to intraspecific variation and differential wear (Fig. 8). In some cases, the metaconid and protoconid share a single, medially positioned and anteroposteriorly directed connection to the anteroconid. Conversely, others feature a connection that is more lingually placed and obliquely directed, resulting in a broader merging of the anteroconid and metaconid. ETMNH 8242 represents the extreme case of the medially placed and anteroposteriorly directed connection (anterior mure), which is distinctly long and prevents the early merger of the metaconid with the anteroconid. ETMNH 16003 and 25983, however, exhibit the opposite pattern, where there is no shared connection between the metaconid and the protoconid. Instead, both cuspids are individually connected to anteroconid, resulting in a distinctly long entoflexid.

In terms of comparisons with modern specimens, ETMNH 8242 closely resembles AMNH 204463, 204464, 204469 and USNM 54396, while ETMNH 16003 and particularly 25983 show greater similarity to USNM 54415 and 54396 (Fig. 7&8). In summary, lower molars of *Neotomodon* from GFS exhibit numerous similarities with those in the modern collection, but they also display some morphological variations that are not adequately represented in the limited modern samples studied here. This suggests that the fossil species may represent a distinct species and have had a different lifestyle than what's been previously documented in extant species.

Fig. 7 Molars of *Neotomodon* sp. from GFS. **A**,**B**,**C**,**D:** occlusal view, **E,F:** labial view. **A.** ETMNH 25983, right m1, **B&E.** 8242, left dentary fragment with m1 and m2 (mirrored for comparison), **C&F**. ETMNH 16013, right dentary fragment with m1, **D**. ETMNH 788, left maxilla fragment with M1

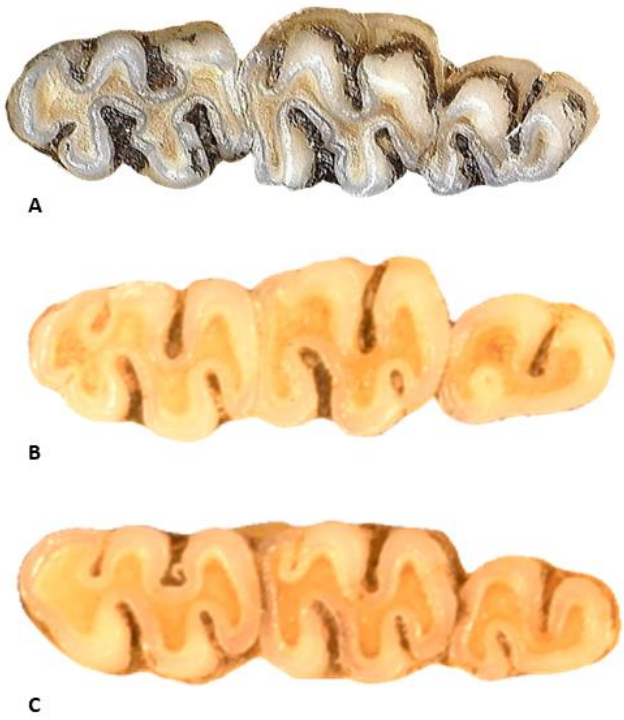

Fig. 8 Tooth rows of lower right molars in modern *Neotomodon* showing variation in occlusal morphology through wear (scaled to the same toothrow length). **A**. AMNH 204464, *Neotomodon alstoni alstoni*; **B**. USNM 54415, *Neotomodon alstoni perotensis*; **C**. USNM 54396, *Neotomodon alstoni perotensis*

Table 4 Measurements (mm) of *Neotomodon* sp. from GFS and other extant taxa. GFS species is highlighted in bold

Dimension / Species	M1-L	M1-W	m1-L	m1-W	m2-L	m2-W	reference
***Neotomodon* sp.**	**1.47**	**1**	**1.54-1.79**	**0.97-1.28**	**1.36**	**1.13**	**GFS, this study**
Neotomodon alstoni alstoni	2.2	1.3	2.15-2.33	1.04-1.5	1.61-2	0.97-1.46	AMNH collection, Hoffmeister 1945
Neotomodon alstoni perotensis	2.02-2.47	1.27-1.49	1.97-2.11	1.18-1.44	1.08-1.53	0.68-0.87	USNM collection

Tribe NEOTOMINI Merriam, 1894

Subtribe NEOTOMINA Merriam, 1894

Genus *NEOTOMA* Say and Ord, 1825

Neotoma sp.

(Fig. 9; Table 5)

Referred Specimens — ETMNH 8222, ETMNH 14697 and 24209, M1; ETMNH 23634, maxilla fragment with right M1 in situ, isolated M1 and M2; ETMNH 36765, M2; ETMNH 36766, two isolated m2.

Description — The M1 is rooted, hypsodont and well preserved with moderate premortem wear (Fig. 9). It is distinctly smaller than other known M1s of *Neotoma* (Table 5). The occlusal 'M' shape pattern is common and there are no accessory structures present. The flexi do not extend to the base of the crown. The anterior wall is generally rounded, while the posterior wall is vertically flat. The anterocone is anteromedially placed and is transversely expanded. All major cusps are widely confluent with connecting lophs and diagonally aligned. The protocone is widely connected to the anterocone and often posterolabially joins the paracone by a short loph positioned close to the midline of the tooth. This loph is notably narrow on the isolated M1 of ETMNH 23634 and disappears on ETMNH 8222. A minute projection on the anteromedial margin of the paracone is the only remnant of this loph connection on ETMNH 23634. With that being said, ETMNH 8222 and 23634 has paraflexus and hypoflexus confluent with one another to some extent because of the absence of such loph. A small enamel fold is only present on the posterior margin of the anterocone of ETMNH 8222.

The paraflexus on two M1s of ETMNH 23634 is more obliquely directed, paralleling the metaflexus and opposing the hypoflexus (Fig. 9). The protoflexus is usually indistinct in four out of five specimens, and appears as a reduced anterior groove or indentation between the anterocone and the protocone. The occlusal surface of ETMNH 24209 does not exhibit the protoflexus, but it persist towards the base of the crown. ETMNH 8222, however, has a prominent protoflexus that distinctly differentiate the anterocone and protocone, allowing the anterocone to be more transversely expanded and the paraflexus first directs transversely then posterolingually (Fig. 9). The hypoflexus is usually anterolabially directed but does not always oppose the paraflexus coming from the labial side (ETMNH 14697 and 24209). The metacone is always posteriorly linked to the hypocone by a posteroloph. An indistinct indentation is present at the posterior margin of the connection of metacone and posteroloph on ETMNH 8222, 23634 and 24209.

The M2 is rooted and also relatively small; it is hypsodont and highly prismatic (Fig. 9). The M2 specimens are well preserved and experienced moderate wear. The anterior crown wall is flat with the posterior wall tapers and less compressed. The anterocone is anteromedially placed and transversely expanded. It is widely confluent with the protocone. A very reduced protoflexus is only present as a shallow groove on the anterior crown wall of ETMNH 23634 to differentiate the protocone and anterocone. Such flexus is unseen on ETMNH 36765. The paracone and protocone loph connection is very reduced on both M2s. This connection is more medially placed on ETMNH 23634 compared to that on ETMNH 36765. The paraflexus is enclosed at the edge of the tooth. A minute stretch of the anterolabial margin of the paracone is present on ETMNH 23634, while a similar projection is located on the anterolingual margin of the hypocone of ETMNH 36765. The paracone and the hypocone are diagonally aligned and

widely confluent. The hypocone is also posteriorly linked to the metacone by the posteroloph. There are no accessory structures present.

The m2 from GFS is rooted and has a distinct 'S' shape of the lophid connections between the cuspids from occlusal view (Fig. 9). There are no accessory structures present in the flexids. The anterior crown wall is always vertically flat, while the posterior wall is rounded. The labial and lingual lophids alternate, with the labial one more anteriorly placed and relatively transversely directed.

Remarks — All specimens of *Neotoma* sp. from GFS consistently exhibit a smaller size in comparison to known records of modern and extinct *Neotoma* (Table 5), but these specimens share several key morphological characters with *Neotoma*. Characteristics features of *Neotoma* have been discussed in many studies (Tomida 1985; Czaplewski 1990; Zakrzewski 1991; Martin and Zakrzewski 2019), which include: 1) widely confluent cusp(id)s and loph(ids), allowing the cusp(id) to be obliquely aligned; 2) the labial flexi are generally postvergent in the same direction, with the provergent metaflexus diagonally opposing the paraflexus; 3) absence of accessory structures; 4) S-shaped occlusal pattern of m2 after a certain degree of wear. Although not explicitly mentioned by many, upper molars of *Neotoma* have a narrow connection between the protocone and the loph structure linking the hypocone and paracone (Fig. 9). This connection can easily disappear with wear, and the change of this connection is reflected on many of our GFS *Neotoma* sp. (Fig. 9). All of these features are evident in the GFS *Neotoma*, but the distinct size may indicate it represents a different species than previously described records.

It is worth noting that the M1 of ETMNH 8222 is morphologically distinct compared to other M1 specimens from GFS. It has a deep protoflexus, a prominently transverse anterocone, the complete loss of the connection between the protocone and paracone, and lacks the

streamlined enamel wall typically observed in *Neotoma*. Nevertheless, the strong tendency of ETMNH 8222 to develop widely confluent and obliquely aligned cusps and lophs is a highly diagnostic characteristic that may outweigh all other minor differences, positioning ETMNH 8222 within *Neotoma* rather than *Neotomodon*.

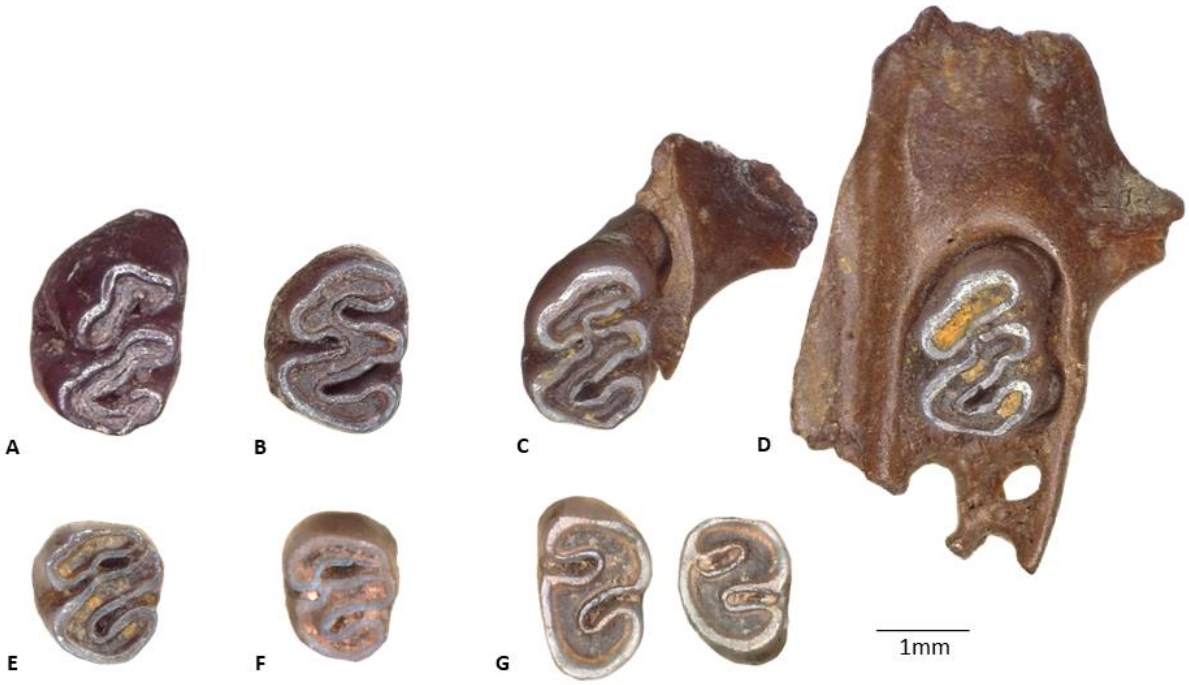

Fig. 9 Upper molars of *Neotoma* sp. from GFS. **A**. ETMNH 8222, left M1; **B**. ETMNH 14697, left M1; **C**. ETMNH 23634, left M1; **D**. ETMNH 23634, right M1 (mirrored for comparison); **E**. ETMNH 23634, left M2; **F**. ETMNH 36965, right M2; **G**. ETMNH 36766, left and right (mirrored for comparison) m2s

Table 5 Measurements (mm) of *Neotoma* sp. from GFS and other extinct taxa. GFS species is highlighted in bold

Dimension / Species	M1-L	M1-W	M2-L	M2-W	m2-L	m2-W	reference
***Neotoma* sp.**	**1.69-1.89**	**1.17-1.34**	**1.32-1.46**	**1.17-1.29**	**1.41-1.72**	**1.18-1.2**	**GFS, this study**
Neotoma (Paraneotoma) minutus†	-	-	2.2	1.7	-	-	Dalquest 1983
Neotoma sawrockensis	-	-	-	-	2.4	1.9	Hibbard 1967
Neotoma fossilis†	2.88-3.18	2.2-2.35	2.24-2.56	1.92-2.04	2.76	2	Tomida 1985, AMNH collection
Neotoma vaughani†	3.41	2.36	2.39-2.52	2.31	2.62	2.03	Czaplewski 1990
Neotoma taylori†	3.3-4.08	2.17-2.67	2.4-3.3	2-2.42	2.58-3.17	1.8-2.42	Tomida 1985, Zakrzewski 1991

Genus *XENOMYS* Merriam, 1897

Xenomys sp.

(Fig. 10)

Referred Specimens — ETMNH 14691, left dentary fragment with m1 and m2; ETMNH 20595, left dentary fragment with m1.

Description — The dentary fragment of ETMNH 14691 preserves only m1 and m2, most of the diastemal ramus, and only partial horizontal ramus that is parallel to the tooth row (Fig. 10). The dentary that is posterior to the posterior alveolus of the m3 is missing. The dentary fragment of ETMNH 20595 only preserves m1 and partial diastemal ramus. The posterior portion of the dentary is missing after the anterior alveolar of m2. From the occlusal view, a minute mental foramen is present on the labial side of the diastemal ramus and just below the anterior root of the m1 there is a possible puncture mark with no known cause (Fig. 10). The tooth row is elevated, exposing partial roots. The anterior masseteric crest ends ventrally to the anterior root of the m1 on the horizontal ramus. The mental foramen is located on the ventrolabial side of the diastemal ramus. Both m1 and m2 are heavily worn but well preserved.

The m1 is anteroposteriorly elongated and relatively narrow (Appendix B), with the crown tapered anterolabially and posterolabially (Fig. 10). The anterior wall is rounded with an anteriorly placed anteroconid that is asymmetrically placed and slightly angled labially (Fig. 10), which lead to a labially curved midline of the tooth. The major cuspids after the anteroconid are alternately placed, with the metaconid being the smallest and the entoconid being the largest. All cuspids are confluent with the lophids. The prominent posterolophid is transversely directed and narrows lingually while being separated from entoconid by a strong posteroflexid. There is no

accessory structure present. The flexids are all wide and deep, although not as deep as reaching the base of the crown. The protoflexid and metaflexid are obliquely opposing each other, while the entoflexid and hypoflexid are provergent and strongly alternated.

The m2 of ETMNH 14691 is wide anteriorly and has a narrowed posterior portion (Fig. 10). The protoconid, the metaconid, and the anterior cingulid are completely merged with each other and share the same anterior margin. The combination of the protoconid and the metaconid results in the presence of a wide dental field that makes up about half of the occlusal surface. The entoconid is widely confluent with this wide dental field anteriorly and with the hypoconid posteriorly. The posterolophid is short but prominent, directing transversely. The protoflexid and metaflexid are absent. The remnant of the posteroflexid is present to separate the posterolophid from the entoconid. Just like the ones on m1, the hypoflexid and the entoflexid alternates on m2 too.

Remarks — Morphology of ETMNH 14691 and 20595 resemble extant *Xenomys* (Fig. 10). That genus is characterized by having: 1) ventral placement of the anterior masseteric crest and the labially placed small mental foramen; 2) distinctly labially bent anterior portion of the m1; 3) two labial and three lingual flexids on m1; 4) transversely directed posterolophid on m1 and m2; 5) wide and deep flexids on m1 and m2 (Merriam 1892a; Cervantes et al. 2016a; Martin and Zakrzewski 2019; Kelly and Martin 2022). The curvature of the tooth is more prominent on ETMNH 20595 than ETMNH 14691. Although the lophids are well developed, they are not long nor robust enough to form distinctly oblique connections between the cuspids, as seen on many other genera like *Neotoma* (Fig. 9&10). Instead, all cuspids are met at about the midline of the tooth as is typical *Xenomys* (Fig. 10A-C). The m1 and m2 of GFS specimens closely resemble *Xenomys* in all the unique morphological characters mentioned above (Fig. 10A-C). Although

Hodomys from *Hodomys-Xenomys* clade also has similar morphology, it is known to occasionally exhibit a shallow reentrant angle on the anterior margin of the anteroconid that is anterolabial to the metaflexid (Fig. 10D; Merriam 1892b; Cervantes et al. 2016b; Kelly and Martin 2022). Even after considerable wear, this reentrant angle is persistent and the lingual margin of the anteroconid retains a pointy shape that is the opposite on *Xenomys* where that lingual margin is distinctly rounded (Fig. 10). Both ETMNH 14691 and 20595 have a more lingually rounded anteroconid. However, the extant *Xenomys* is larger than *Xenomys* sp. from GFS (Fig. 10). Additionally, there is no m3 preserved to confirm if *Xenomys* sp. has the same signature 'S' shape m3 as those of *Hodomys-Xenomys* clade have (Kelly and Martin, 2022). As such, until further materials from different tooth positions are recovered, ETMNH 20595 and 14691 are identified as *Xenomys* sp., though additional materials could warrant re-evaluation.

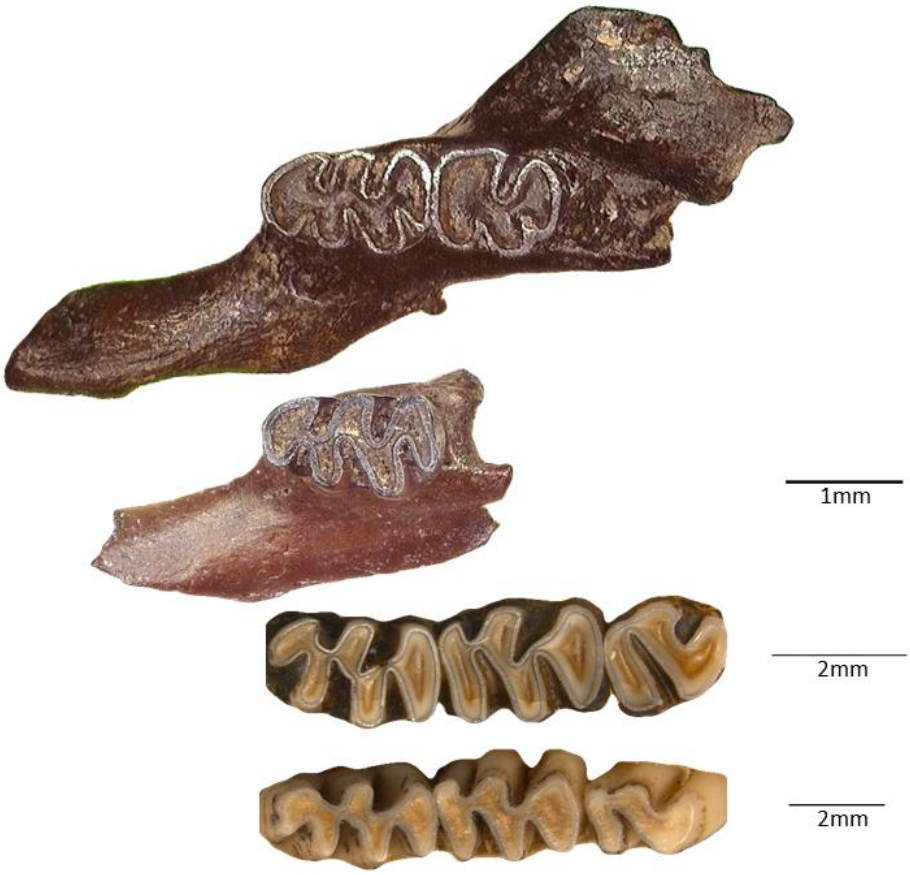

Fig. 10 Dentary of *Xenomys* sp. from GFS and modern *Xenomys* and *Hodomys* specimens. **A**. ETMNH 14691, left dentary fragment with m1 and m2 (mirrored for comparison); **B**. ETMNH 20595, left dentary fragment with m1; **C**. *Xenomys nelsoni* specimen from (Cervante et al. 2016a); **D**. *Hodomys alleni* specimen (Cervante et al. 2016b)

CHAPTER 4. DISCUSSION

Study of the cricetids from GFS revealed eight distinct taxa from seven genera, including: *Postcopemys* sp. large and small, Oryzomyini, *Symmetrodontomys* sp., *Peromyscus* sp., *Neotomodon* sp., *Neotoma* sp., and *Xenomys* sp. Among these cricetid taxa at GFS, five out of eight are brachydont, two are hypsodont (*Neotoma* sp. and *Xenomys* sp.) and one is mesodont (*Neotomodon* sp.). The GFS cricetid assemblage displays a wide range of body sizes and crown heights, reflecting GFS having the capacity to meet diverse dietary preferences and provide available niches. GFS primarily hosted brachydont cricetids, supporting the inference of a paleo-forest environment with predominantly omnivorous species, devoid of grass-feeding or aquatic-adapted cricetids.

The modern Tennessean cricetid include five genera (8 species) of Neotominae, two genera of Sigmodontinae, and four genera (7 species) of Arvicolinae (Appendix C). The fossil record at GFS partially aligns with the modern one, featuring one sigmodontine (Oryzomyini) taxon and two neotomine (*Peromyscus* and *Neotoma*) genera shared. However, GFS includes two more neotomine genera (*Neotomodon* and *Xenomys*), which are not typical for the region. Smaller extant neotomines, such as *Reithrodontomys* and *Ochrotomys*, are absent at GFS, but their niches may have been filled by the small *Postcopemys* and *Peromyscus* in the past. Interestingly, the most common cricetid, *Postcopemys* sp. large, is substantially larger in size than any the brachydont generalists inhabiting the region today.

Despite the presence of arvicoline taxa with hypselodont dentition in modern Tennessee, such as muskrats and various vole species (Appendix C), no related taxa were found at GFS during the early Pliocene. Arvicolines (voles, lemmings, and muskrats) are both diverse and abundant in modern communities, but their absence from GFS (to date) possibly reflects

differential conditions in the past that meant the niches they currently occupy did not exist in the area at the time. Another explanation for the absence of arvicolines is that though present elsewhere in North America in the early Pliocene they may not have dispersed to the forests of the Appalachians until later.

With eight taxa, GFS is the most cricetid species-rich site in eastern North America during the early Pliocene. In comparison, the contemporaneous Pipe Creek Sinkhole in Indiana only recovered two cricetid species, with only one overlapping taxon (*Symmetrodontomys*, Martin, Goodwin et al. 2002). Other notable sites in the east from the Pliocene (late Blancan), such as Haile 15A and Inglis 1A/1C in Florida, primarily yielded higher crowned cricetids like *Sigmodon* (Ruez 2001, 2009). Meanwhile, prolific sites in central and western North America, such as the Hagerman Fauna (Glenns Ferry Formation) in Idaho, Beck Ranch in Texas, and Rexroad and Deer Park faunas in Kansas, tend to yield more higher crowned arvicolines (*Cosomys*, *Nebraskomys*, *Ogmodontomys*, *Ophiomys*, and *Ondatra*), *Sigmodon*, smaller-sized neotomines like *Reithrodontomys* and *Baiomys*, *Onychomys*, and taxa like *Bensonomys* that are phylogenetically closer to *Symmetrodontomys* (Hibbard 1941, 1967; Zakrzewski 1969; Martin, Honey et al. 2002; Martin 2008; Ruez and Gensler 2008; Ruez 2009; Ronez et al. 2021).

What makes GFS truly unique among eastern faunas is the presence of *Postcopemys*, a taxon previously reported only from sites in western (Verde Formation in Arizona, Dove Spring Formation in California) and southern (Chapala Formation in Mexico) North America, and typically late Hemphillian early Blancan in age (Jacobs 1977; Czaplewski 1990; Lindsay and Czaplewski 2011; May 2011; Lindsay and Whistler 2014; Rincón et al. 2016). Additionally, the co-occurrence of two distinct neotomines which are restricted to Mexico now, *Xenomys* and *Neotomodon*, further emphasizes the exceptional nature and diverse origins of the GFS cricetid

fauna. Occurrences of *Neotomodon* and *Xenomys*, like the previously described records of *Heloderma* and *Notolagus lepusculus* from the Gray Fossil Site (Mead et al. 2012, Samuels and Schap 2021), suggest a connection of site's fauna to lower latitude faunas from the southwest United States and Mexico.

Character State Analysis

Postcopemys – All upper molars of *Postcopemys* sp. large and small from GFS consistently have alternating cusps, relatively straight loph connections between cusps, and isolated posterior cingula. The mesoloph, mesostyle, and parastyle are rather common on M1 and M2 too: 90% of the specimens have mesostyle, all have mesoloph, but some are longer and reaching the edge of the tooth, all M1s have parastyle. Although these three characters are more variably present on *Postcopemys* and *Paronychomys*, *Postcopemys* is more consistent with having the mesoloph/mesostyle structure, as well as the general loph direction going anteroposteriorly, which may result in the lack of alignment, or subalignment, of protolophule II and anterior arm of hypocone.

Lower molars of *Postcopemys* sp. large lack mesolophid and other accessory structures, but consistently have the lingual connection between the anteroconid and the metaconid. Solely looking at these characters may place these lower molars from GFS closer to *Paronychomys*. However, lower molars of *Paronychomys* are similar to their upper molars and tend to have a stronger alignment of the posterior arm of protoconid and the entolophid, even though the lophid connections on the lower molars are less obliquely aligned as the upper ones (Jacobs 1977; Kelly 2013; Kelly and Martin 2022).

Symmetrodontomys – The upper molar of *Symmetrodontomys* sp. from GFS has more complex flexus with more accessory structures like paracone and mesoloph strongly present. The distinct

anterobasal shelf with an anterostyle on top is a character shared by *Symmetrodontomys* sp. and *Bensonomys*. However, accessory structures after the anteroconid are significantly reduced. Only about 37% of *Bensonomys* species studied have parastyle, 10% develop an enamel lake, and less than 50% have a mesoloph (Appendix G). *Jacobsomys* have more frequent occurrences of accessory structures in the flexi. Nevertheless, none of *Jacobsomys* species studied have anterobasal shelf with the anterostyle (Appendix G). Compared to these two genera, *Symmetrodontomys* is more consistent with all characters present in GFS *Symmetrodontomys* sp., with the exception of previous records of *Symmetrodontomys* have a more opposite placement of the cusps.

The lower molars from GFS have similar expressions of the characteristics among them. The records of *Symmetrodontomys* have more individually varied presence of accessory structures like stylids in the flexids and the mesolophid. What used to be considered as the signature of *Symmetrodontomys*, the strong bifurcation of the anteroconid and the symmetrical placement of cuspids, are no longer considered to be unique characters when compared to other similar-size genera like *Bensonomys* and *Jacobsomys*. In fact, these characters in these genera can be even more prominent: about 50% of *Bensonomys* species have strongly opposing cuspids, almost all recorded *Bensonomys* and *Jacobsomys* have anteroconid more strongly bifurcated (Appendix G). What truly distinguishes the previous record of *Symmetrodonomys* and *Symmetrodontomys* sp. from GFS is the length of the anterior mure and position of the protoconid and the metaconid. All *Symmetrodonomys* and *Symmetrodontomys* sp. from GFS have short to no anterior mure that allows the formation of 'X' shaped pattern among the anteroconid, protoconid and the metaconid. Although two out of three examined species of

Jacobsomys have a tendency to develop such character, *Bensonomys* consistently have longer anterior mure and less anteriorly oriented protoconid and metaconid.

Peromyscus – *Peromyscus* is a very diverse group of brachydont cricetids and has a long history in North America (Lindsay 2008, Martin and Kelly 2023). Hence, many taxa were previously misplaced in this genus until more materials became available and detailed examination reallocated them to other genera. Morphological variation among individuals of *Peromyscus* sp. from GFS is very common too. The alternation of the cusps and the presence of mesolophid are some of the most variable characters. 60% of the specimens have a long mesolophid reaching the edge of the tooth, and all specimens show cusp alternation to different degrees (Fig. 6). This is the situation also seen on other *Peromyscus* species from the collection and the literature. Thus, morphology alone is not enough to classify *Peromyscus* sp. from GFS to any particular species. Although the size of *Peromyscus* sp. fall within the range *Peromyscus*, many *Peromyscus* species have overlapped size ranges.

Oryzomyini – Assigning the fairly worn specimen (ETMNH 32961) to a specific taxon beyond the tribe poses a considerable challenge. When compared to Oryzomyini from GFS, 33% of *Oryzomys* m1s from previous records has slightly alternated cusps, 67% has bifurcated anteroconid on m1, about 67% has ectostylid, almost all have strong mesolophid, and less than 17% has a posteriorly directed posterolophid (Appendix I). As such, Oryzomyini from GFS typically demonstrate simple, wide, and deep flexids, devoid of many accessory structures. Even the presence of a few accessory structures, such as the ectolophid, cannot be reliably confirmed as persistent traits the population of Oryzomyini from GFS. Oryzomyini from GFS mostly resembles *Zygodontomys* morphologically, however the relatively higher crown and the

orientation of the cusp may eventually exclude GFS specimens from being assigned to this genus.

Biostratigraphic Implications

Paleontological findings at GFS reveals a diverse array of eight taxa, some of which exhibit a notable presence in other contemporaneous sites (Kelly and Martin, 2023). Among these taxa, *Peromyscus* and *Neotoma* stand out for their frequent appearances in many early Blancan sites and their continuous distribution into modern times (e.g., Ruez 2001; Martin, Martin, Honey et al. 2002; Martin 2005; Mou 2011). In contrast, certain other taxa identified at GFS have been restricted to a limited geographic range. For instance, *Postcopemys* was previously documented in late Hemphillian Yepómera fauna in Mexico (Rincón et al 2016), early Blancan Warren fauna in South California (May et al. 2011) and Verde fauna in Arizona (Czaplewski 1990; Lindsay and Czaplewski 2011), but now demonstrates a lineage in the Appalachian region. Similarly, the fossil record of *Xenomys*, previously confined to early Pliocene El Ocote fauna in Mexico (Carranza-Castañeda and Walton 1992; Martin and Zakrzewski 2019; Martin and Kelly 2023), now extends into contemporaneous Gray in the Appalachians.

In addition to broadening the geographic ranges of the Pliocene taxa mentioned above, the cricetid assemblage at GFS also advances fossil records of other genera stratigraphically (Fig. 11). The fossil range of *Neotomodon* has expanded from the late Pleistocene southern Mexico (Alvarez 1966; Cruz-Muñoz et al. 2009; Ferrusquía-Villafranca et al. 2010) to early Pliocene Appalachian deposits. *Symmetrodontomys*, only previously known from Indiana and Kansas with the earliest record dated back to about 4.75 Ma (Martin, Goodwin et al. 2002; Martin, Honey et al. 2002; Martin et al. 2008; Martin and Kelly 2023), is now identified from the GFS deposits

and thus advances our understanding of the history of this genus to 4.9Ma from southeastern North America. The earliest occurrence of *Symmetrodontomys* in the early Pliocene, along with that of *Neotoma* and *Peromyscus*, corresponds with the rabbit data and extinction of rhinos as well as the occurrence of *Plionarctos* at the site (Bell et al. 2004; Wallace and Wang 2004; Samuels et al. 2018; Samuels and Schap 2021; Kelly and Martin 2023).

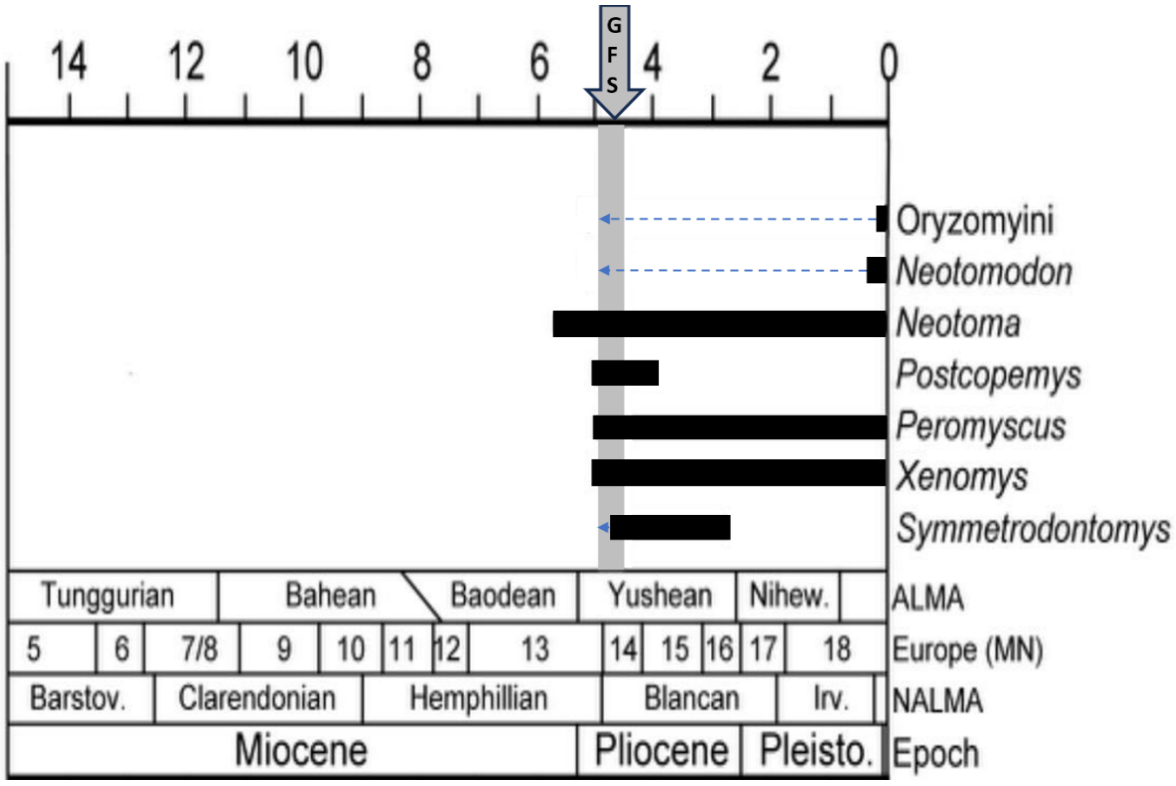

Fig. 11 Biochronology of cricetid genera from GFS. Age range is modified from Martin et al (2008), Ferrusquía-Villafranca et al. (2010), and Martin and Kelly (2023). Blue arrow dash lines indicate the advance of previous fossil records of certain genera; gray vertical bar indicates the age range of GFS (Samuels et al. 2018; Samuels and Schap 2021); black horizontal bars indicate the age range of fossil record

CHAPTER 5. CONCLUSION

As one of the few pre-Pleistocene sites in eastern North America with a record of cricetids, Gray Fossil Site (GFS) in northeastern Tennessee stands out for its remarkable preservation of a diverse cricetid fauna. The study revealed eight distinct cricetid taxa from GFS, including *Postcopemys* (two species), *Symmetrodontomys*, Oryzomyini, *Peromyscus*, *Neotomodon*, *Neotoma*, and *Xenomys*. The unique co-occurrence of common Pliocene cricetid taxa and two more unusual and rare taxa, *Xenomys* and *Neotomodon*, render GFS the most cricetid species-rich site during the early Pliocene. Furthermore, even those taxa commonly found from contemporaneous sites have a strong tendency to develop unique morphological characters or distinctly large size at the GFS, setting them apart from any known species. Although some conical hypsodont taxa are present, GFS predominantly hosted brachydont cricetids, supporting the hypothesis of a paleo-forest environment with predominantly omnivorous species. As such, the cricetids at GFS play a critical role in understanding the biodiversity and evolutional history of a large group of small mammals in North America during the Late Neogene, including lineages that persists into the present day. It is important to note, however, that the diminutive nature of cricetid materials makes it challenging to collect more complete and associated specimens, which would be necessary for refining some identifications to the species-level and confirming the presence of new species.

REFERENCES

Alvarez ST. 1966. Roedores fósiles del Pleistoceneo de Tequesquinahua, Estadode México. Acta Zool. Mex. 8(3):1–16.

Baskin JA. 1978. *Bensonomys*, *Calomys*, and the origin of the phyllotine group of Neotropical cricetines (Rodentia: Cricetidae). J. Mammal. 59(1):125-135. https://doi.org/10.2307/1379882

Baskin JA. 1979. Small mammals of the Hemphillian age White Cone Local Fauna, Northeastern Arizona. J. Paleontol. 53(3):695-708.

Baskin JM, Baskin CC. 2016. Origins and relationships of the mixed mesophytic forest of Oregon-Idaho, China, and Kentucky: Review and Synthesis. Ann. Missouri Bot. Gard. 101(3):525-552. https://doi.org/10.3417/2014017

Bell CJ, Lundelius EL, Barnosky AD, Graham RW, Lindsay EH, Ruez DR, Semken HA, Webb SD, Zakrzewski RJ. 2004. Late Cretaceous and Cenozoic mammals of North America: biostratigraphy and geochronology. New York (NY): Columbia University Press. The Blancan, Irvingtonian, and Rancholabrean Mammal Ages; p. 232-314.

Boardman GS, Schubert BW. 2011. First Mio-Pliocene salamander fossil assemblage from the southern Appalachians. Palaeontol. Electron.14(2):16A.

Bourque JR, Schubert BW. 2015. Fossil musk turtles (Kinosternidae, *Sternotherus*) from the Late Miocene–Early Pliocene (Hemphillian) of Tennessee and Florida. J. Vertebr. Paleontol. 35(1):1-19. https://doi.org/10.1080/02724634.2014.885441

Cervantes FA, Castañón CE, Sánchez JA, Vargas J, Hortelano Y. 2016a. Molares de la mandíbula inferior derecha de la rata arborícola *Hodomys alleni*. Mexico: Irekani; [issued 2014 March 14; accessed 2023 October 6] http://unibio.unam.mx/irekani/handle/123456789/37951?proyecto=Irekani

Cervantes FA, Castañón CE, Sánchez JA, Vargas J, Hortelano Y. 2016b. Molares de la mandíbula inferior derecha de la rata de Magdalena *Xenomys nelsoni*. Mexico: Irekani; [issued 2016 May 27; accessed 2023 October 6]. http://unibio.unam.mx/irekani/handle/123456789/37950?proyecto=Irekani

Carleton MD, Musser GG. 1984. Muroid rodents. In: Anderson S, Jones Jr. J, editors. Orders and families of recent mammals of the world. New York (NY): J. Knox Jones Jr. p. 255-265.

Carranza-Castañeda O. 1992. Cricetid rodents from the Rancho El Ocote fauna, late Hemphillian (Pliocene), State of Guanajuato. Revista, volumen. 10(1):71-93.

Cruz-Muñoz V, Arroyo-Cabrales J, Graham RW. 2009. Rodents and lagomorphs from the Late Pleistocene deposits at Valsequillo, Puebla, México. Current Research in the Pleistocene. 26:147–149.

Czaplewski NJ. 1987. Sigmodont rodents (Mammalia; Muroidea; Sigmodontinae) from the Pliocene (early Blancan) Verde Formation, Arizona. J. Vertebr. Paleontol. 7(2):183-199. https://doi.org/10.1080/02724634.1987.10011652

Czaplewski NJ. 1990. The Verde local fauna: small vertebrate fossils from the Verde Formation, Arizona. San Bernardino County Museum Association. 37(3):1-39.

Dalquest WW. 1978. Early Blancan mammals of the Beck Ranch local fauna of Texas. J. Mammal. 59(2):269-298. https://doi.org/10.2307/1379912

DeSantis LR, Wallace SC. 2008. Neogene forests from the Appalachians of Tennessee, USA: geochemical evidence from fossil mammal teeth. Palaeogeogr. Palaeoclimatol. Palaeoecol. 266(1-2):59-68. https://doi.org/10.1016/j.palaeo.2008.03.032

Doughty EM, Wallace SC, Schubert BW, Lyon LM. 2018. First occurrence of the enigmatic peccaries *Mylohyus elmorei* and *Prosthennops serus* from the Appalachians: latest Hemphillian to Early Blancan of Gray Fossil Site, Tennessee. PeerJ. 6:e5926.

Edwards EJ, Osborne CP, Strömberg CA, Smith SA, C4 Grasses Consortium, Bond WJ, Christin PA, Cousins AB, Duvall MR, Fox DL, Freckleton RP. 2010. The origins of C4 grasslands: integrating evolutionary and ecosystem science. Science. 328(5978):587-591.

Fabre PH, Hautier L, Dimitrov D, P Douzery EJ. 2012. A glimpse on the pattern of rodent diversification: a phylogenetic approach. BMC Evol. Biol. 12(1):1-9. https://doi.org/10.1186/1471-2148-12-88

Ferrusquía-Villafranca I, Arroyo-Cabrales J, Martínez-Hernández E, Gama-Castro J, Ruiz González J, Polaco OJ, Johnson E. 2010. Pleistocene mammals of Mexico: A critical review of regional chronofaunas, climate change response and biogeographic provinciality. Quat. Int. 217(1-2):53-104.

Graham A. 1999. Late Cretaceous and Cenozoic history of North American vegetation: north of Mexico. Oxford University Press. https://doi.org/10.1093/oso/9780195113426.001.0001

Hershkovitz P. 1971. A new rice rat of the *Oryzomys palustris* group (Cricetinae, Muridae) from Northwestern Colombia, with Remarks on Distribution. J. Mammal. 52(4):700-709. https://doi.org/10.2307/1378917

Hibbard CW. 1941. Mammals of the Rexroad fauna from the upper Pliocene of southwestern Kansas. Trans. Kans. Acad. Sci. (1903-). 44:265-313. https://doi.org/10.2307/3624893

Hibbard CW. 1949. Techniques of collecting microvertebrate fossils. Ann Arbor: University of Michigan Press. 8(2):7-19.

Hibbard CW. 1962. Two new rodents from the early Pleistocene of Idaho. J. Mammal. 43(4):482-485. https://doi.org/10.2307/1376911

Hibbard CW. 1967. New rodents from the late Cenozoic of Kansas. Papers of the Michigan academy of science, arts, and letters; 1966; unknown, MI. Unknown (MI): Michigan Academy of Science, Arts and Letters. 52.

Hoffmeister DF. 1945. Cricetine rodents of the middle Pliocene of the Mulholland Fauna, California. J. Mammal. 26(2):186-191. https://doi.org/10.2307/1375095

Hulbert RC, Wallace SC, Klippel WE, Parmalee PW. 2009. Cranial morphology and systematics of an extraordinary sample of the Late Neogene dwarf tapir, *Tapirus polkensis* (Olsen). J. Paleontol. 83(2):238-262. https://doi.org/10.1666/08-062.1

Jasinski SE, Moscato DA. 2017. Late Hemphillian colubrid snakes (Serpentes, Colubridae) from the Gray Fossil Site of Northeastern Tennessee. J. Herpetol. 51(2):245. https://doi.org/10.1670/16-020

Jacobs LL. 1977. Rodents of the Hemphillian Age Redington Local Fauna, San Pedro Valley, Arizona. J. Paleontol. 51(3):505-519.

James GT. 1963. Paleontology and nonmarine stratigraphy of the Cuyama Valley Badlands, California. Oakland (CA): University of California Press.

Keenan SW, Engel AS. 2017. Reconstructing diagenetic conditions of bone at the Gray Fossil Site, Tennessee, USA. Palaeogeogr. Palaeoclimatol. Palaeoecol. 471:48-57. https://doi.org/10.1016/j.palaeo.2017.01.037

Kellogg L. 1910. Rodent fauna of the late Tertiary beds at Virgin Valley and Thousand Creek, Nevada. Univ. Calif. Publ., Bull. Dep. Geol. 5(29):421-437.

Kelly TS. 2013. New Hemphillian (late Miocene) rodents from the Coal Valley Formation, Smith Valley, Nevada. Paludicola. 9(2):70-96.

Kelly TS, Whistler DP. 2014. New late Miocene (latest Clarendonian) to early Hemphillian cricetid rodents from the upper part of the Dove Spring Formation, Mojave Desert, California. Paludicola. 10:1-48.

Kelly TS, Martin RA. 2022. Phylogenetic positions of *Paronychomys* Jacobs and *Basirepomys* Korth and De Blieux relative to the tribe Neotomini (Rodentia, Cricetidae). J. Paleontol. 96(3):692-705. https://doi.org/10.1017/jpa.2021.121

Kelly TS, Martin RA, Ronez C, Cañón C, Pardiñas UF. 2022. Morphology and genetics of grasshopper mice revisited in a paleontological framework: reinstatement of

Onychomyini (Rodentia, Cricetidae). J. Mammal. 104(1):3-28. https://doi.org/10.1093/jmammal/gyac093

Korth WW. 1998. Rodents and lagomorphs (Mammalia) from the late Clarendonian (Miocene) Ash Hollow Formation, Brown County, Nebraska. Ann. Carnegie Mus. 67:299-348. https://doi.org/10.5962/p.215209

Korth WW, De Blieux DD. 2010. Rodents and lagomorphs (Mammalia) from the Hemphillian (late Miocene) of Utah. J. Vertebr. Paleontol. 30(1):226-235. https://doi.org/10.1080/02724630903412448

Korth WW. 2011. New species of cricetid rodents (Mammalia) from the late Miocene (Hemphillian) previously referred to *Peromyscus pliocenicus* Wilson. Ann. Carnegie 1Mus. 79(2):137-147.

Lindsay EH. 1972. Small mammal fossils from the Barstow Formation, California. Univ. Calif. Publ. Geol. Sci. 93:1104.

Lindsay EH. 2008. Cricetidae. In: Janis CM, Gunnell GF, Uhen MD, editors. Evolution of Tertiary mammals of North America. Cambridge (NY): Cambridge University Press. 2:456-479. https://doi.org/10.1017/CBO9780511541438

Lindsay EH, Czaplewski NJ. 2011. New rodents (Mammalia, Rodentia, Cricetidae) from the Verde fauna of Arizona and the Maxum fauna of California, USA, early Blancan land mammal age. Palaeontol. Electron. 14(3):16.

Martin LD. 1980. The early evolution of the Cricetidae in North America. Paleont. Contr. Paper 102.

Martin RA, Goodwin HT, Farlow JO. 2002. Late Neogene (Late Hemphillian) rodents from the Pipe Creek Sinkhole, Grant County, Indiana. J. Vertebr. Paleontol. 22(1):137-151.

Martin RA, Honey JG, Peláez-Campomanes P, Goodwin HT, Baskin JA, Zakrzewski RJ. 2002. Blancan lagomorphs and rodents of the Deer Park assemblages, Meade County, Kansas. J. Paleontol. 76(6):1072-1090.

Martin RA. 2005. Preliminary correlation of Florida and central Great Plains Pliocene and Pleistocene mammalian local faunas based on rodent biostratigraphy. Cenozoic Vertebrates of the Americas: Papers to Honor S. David Webb. Bull. Fla. Mus. Nat. Hist. 45(4):363-367.

Martin RA. 2008. Arvicolidae. In: Janis CM, Gunnell GF, Uhen MD, editors. Evolution of Tertiary mammals of North America. Cambridge (NY): Cambridge University Press. 2:480-497. https://doi.org/10.1017/CBO9780511541438

Martin RA, Peláez-Campomanes P, Honey JG, Fox DL, Zakrzewski RJ, Albright LB, Lindsay EH, Opdyke ND, Goodwin HT. 2008. Rodent community change at the Pliocene Pleistocene transition in southwestern Kansas and identification of the *Microtus* immigration event on the Central Great Plains. Palaeogeogr. Palaeoclimatol. Palaeoecol. 267(3-4):196-207. https://doi.org/10.1016/j.palaeo.2008.06.017

Martin RA, Peláez-Campomanes P, Viriot L. 2018. First report of rodents from the late Hemphillian (late Miocene) Zwiebel Channel and a revised late Neogene

biostratigraphy/biochronology of the Sand Draw area of Nebraska. Hist. Biol. 30(5):636 645. https://doi.org/10.1080/08912963.2017.1313251

Martin RA, Zakrzewski RJ. 2019. On the ancestry of woodrats. J. Mammal. 100(5):1564-82. https://doi.org/10.1093/jmammal/gyz105

Martin RA, Kelly TS. 2023. Biostratigraphy and biochronology of late Cenozoic North American rodent assemblages. Palaeontol. Electron. 26(2):1-29. https://doi.org/10.26879/1303

Martínez-Chapital ST, Schnell GD, Sánchez-Hernández C, Romero-Almaraz MD. 2017. *Sigmodon mascotensis* (Rodentia: Cricetidae). Mamm. Species. 49(954):109-118.

May SR, Woodburne MO, Lindsay EH, Albright LB, Sarna-Wojcicki A, Wan E, Wahl DB. 2011. Geology and mammalian paleontology of the Horned Toad Hills, Mohave Desert, California, USA. Palaeontol. Electron. 14(3):1-63.

Mead JI, Schubert BW, Wallace SC, Swift SL. 2012. Helodermatid lizard from the Mio-Pliocene oak-hickory forest of Tennessee, eastern USA, and a review of monstersaurian osteoderms. Acta Palaeontol. Pol. 57(1):111-121. http://doi.org/10.4202/app.2010.0083

Merriam CH. 1892a. Description of a new genus and species of murine rodent (*Xenomys nelsoni*) from the state of Colima, western Mexico: Proceedings of the Biological Society of Washington. 7:159-163.

Merriam CH. 1892b. Descriptions of nine new mammals collected by E. W. Nelson in the states of Colima and Jalisco, Mexico: Proceedings of the Biological Society of Washington. 7:164–174.

Merriam CH. 1898. A new genus (*Neotomodon*) and three new species of murine rodents from the mountains of southern Mexico. Proc. Biol. Soc. Wash. 12:127-129.

Mou Y. 2011. Cricetid rodents from the Pliocene Panaca Formation, southeastern Nevada, USA. Palaeontol. Electron. 14(3):1-53.

Nowak RM. 1999. Walker's Mammals of the World. Baltimore (MD): Johns Hopkins University Press. http://doi.org/10.56021/9780801857898

Ochoa D, Zavada MS, Liu Y, Farlow JO. 2016. Floristic implications of two contemporaneous inland upper Neogene sites in the eastern US: Pipe Creek Sinkhole, Indiana, and the Gray Fossil Site, Tennessee (USA). Palaeobiodivers. Palaeoenviron. 96:239-254. http://doi.org/10.1007/s12549-016-0233-4

Rincón AD, Czaplewski NJ, Montellano-Ballesteros M, Benammi M. 2016. New Species of *Postcopemys* (cricetidae: Rodentia) from the Early Pliocene of Lago De Chapala, Jalisco, Mexico. Southwest. Nat. 61(2):108-118.

Ronez C, Martin RA, Pardiñas UF. 2020. Morphological revision of *Copemys loxodon*, type species of the Miocene cricetid *Copemys* (Mammalia, Rodentia): a key to understanding the history of New World cricetids. J. Vertebr. Paleontol. 40(2):e1772273.

Ronez C, Martin RA, Kelly TS, Barbière F, Pardiñas UFJ, Ronez C, Martin RA, Kelly TS, Barbière F, Pardiñas UFJ. 2021. A brief critical review of sigmodontine rodent origins, with emphasis on paleontological data. Mastozool. Neotrop. 28(1):495-495. http://doi.org/10.31687/saremMN.21.28.1.0.07

Ronez C, Carrillo-Briceño JD, Hadler P, Sánchez-Villagra MR, Pardiñas UF. 2023. Pliocene sigmodontine rodents (Mammalia: Cricetidae) in northernmost South America: test of biogeographic hypotheses and revised evolutionary scenarios. R. Soc. Open Sci. 10(8):221417. http://doi.org/10.1098/rsos.221417

Ruez Jr DR. 2001. Early Irvingtonian (Latest Pliocene) rodents from Inglis 1C, Citrus County, Florida. J. Vertebr. Paleontol. 21(1):153-171.

Ruez Jr DR, Gensler PA. 2008. An unexpected early record of *Mictomys vetus* (Arvicolinae, Rodentia) from the Blancan (Pliocene) Glenns Ferry Formation, Hagerman Fossil Beds National Monument, Idaho. J. Vertebr. Paleontol. 82:638-642.

Ruez Jr DR. 2009. Revision of the Blancan (Pliocene) mammals from Hagerman Fossil Beds National Monument, Idaho. J. Idaho Acad. Sci. 45(1):1-44.

Samuels JX, Hopkins SS. 2017. The impacts of Cenozoic climate and habitat changes on small mammal diversity of North America. Glob. Planet. Change. 149:36-52. http://doi.org/10.1016/j.gloplacha.2016.12.014

Samuels JX, Bredehoeft KE, Wallace SC. 2018. A new species of *Gulo* from the Early Pliocene Gray Fossil Site (Eastern United States); rethinking the evolution of wolverines. PeerJ. 6:e4648.

Samuels JX, Schap J. 2021. Early Pliocene leporids from the Gray Fossil Site of Tennessee. Eastern Paleontologist. 8:1-23.

Short, Rachel A., Steven C. Wallace, and Laura G. Emmert. 2019. A new species of *Teleoceras* (Mammalia, Rhinocerotidae) from the late Hemphillian of Tennessee. Bull. Fla. Mus. Nat. Hist. 56(5):183-260.

Shunk AJ, Driese SG, Dunbar JA. 2009. Late Tertiary paleoclimatic interpretation from lacustrine rhythmites in the Gray Fossil Site, northeastern Tennessee, USA. J. Paleolimnol. 42:11-24. http://doi.org/10.1007/s10933-008-9244-0

Skinner MF, Hibbard CW, Gutentag ED, Smith GR, Lundberg JG, Holman JA, Feduccia A, Rich PV. 1972. Early Pleistocene pre-glacial and glacial rocks and faunas of north-central Nebraska. Bull. Am. Mus. 148(1).

Solorzano A, Rincón AD, McDonald HG. 2015. A new mammal assemblage from the Late Pleistocene El Breal de Orocual, northeast of Venezuela. La Brea and beyond: The paleontology of Asphalt-preserved biotas. 42:125-150.

Steppan SJ, Adkins RM, Anderson J. 2004. Phylogeny and divergence-date estimates of rapid radiations in muroid rodents based on multiple nuclear genes. Syst. Biol. 53(4):533-553. https://doi.org/10.1080/10635150490468701

Strömberg CA. 2011. Evolution of grasses and grassland ecosystems. Annu. Rev. Earth Planet Sci. 39:517-544. https://doi.org/10.1146/annurev-earth-040809-152402

Tomida Y. 1985. Small Mammal Fossils and Correlation of Continental Deposits, Safford and Duncan Basins, Arizona [Doctor's thesis]. The University of Arizona.

Turvey ST, Weksler M, Morris EL, Nokkert M. 2010. Taxonomy, phylogeny, and diversity of the extinct Lesser Antillean rice rats (Sigmodontinae: Oryzomyini), with description of a new genus and species. Zool. J. Linn. Soc. 160(4):748–772. https://doi.org/10.1111/j.1096-3642.2009.00628.x

Voss R. 1991. An introduction to the neotropical muroid rodent genus *Zygodontomys*. Bull. Am. Mus. Nat. Hist. 210:1-113.

Voss RS, Gómez-Laverde M, Pacheco V. 2002. A new genus for *Aepeomys fuscatus* Allen, 1912, and *Oryzomys intectus* Thomas, 1921: enigmatic murid rodents from Andean cloud forests. Am. Mus. Novit. 2002(3373):1-42.

Wallace SC, Wang L. 2004. Two new carnivores from an unusual late Tertiary forest biota in eastern North America. Nat. 431(7008):556–559. https://doi.org/10.1038/nature02819

Wallace SC. 2011. Advanced members of the Ailuridae (lesser or red pandas–subfamily Ailurinae). In: Glatston AR, editor. Red Panda. William Andrew Publishing. p. 43-60. https://doi.org/10.1016/B978-1-4377-7813-7.00004-5

Weksler M. 2006. Phylogenetic relationships of oryzomine rodents (Muroidea: Sigmodontinae): separate and combined analyses of morphological and molecular data. Bull. Am. Mus. Nat. Hist. 2006(296):1-149.

Zakrzewski RJ. 1969. The rodents from the Hagerman local fauna, upper Pliocene of Idaho [Doctoral dissertation]. Ann Arbor (MI): University of Michigan. 23(1):1-36 p.

Zakrzewski RJ. 1991. New species of Blancan woodrat (Cricetidae) from north-central Kansas. J. Mammal. 72(1):104-109. http://doi.org/10.2307/1381984

Zijlstra JS, McFarlane DA, Van Den Hoek Ostende LW, Lundberg J. 2014. New rodents (Cricetidae) from the Neogene of Curaçao and Bonaire, Dutch Antilles. Palaeontology 57(5):895-908. http://doi.org/10.1111/pala.12091

APPENDICES

Appendix A: Comparative Sample of Extant and Fossil Species Examined in This Study. The Classification Follows Ronez et al. (2021)

Subfamily	Genus	Species	References	Source
Cricetidae incertae sedis				
	Postcopemys	*vasquezi*	Jacobs 1977	Literature
	Postcopemys	sp.; cf. *P. valensis*	Kelly & Whistler 2014	Literature
	Postcopemys	*valensis*	May et al. 2011	Literature
	Postcopemys	sp. *A*	Kelly 2013	Literature
	Postcopemys	sp. *B*	Kelly 2013	Literature
	Postcopemys	*repenningi*	Lindsay & Czaplewski 2011	Literature
	Postcopmeys	*maxumensis*	Lindsay & Czaplewski 2011	Literature
	Postcopemys	*chapalensis*	Rincón et al. 2016	Literature
	Symmetrodontomys	*daamsi*	Martin, Goodwin et al. 2002; Martin, Honey et al. 2002	Literature
	Symmetrodontomys	*simplicidens*	Hibbard 1941; Martin, Honey et al. 2002;	Literature
	Bensonomys	sp.	Kelly & Whistler 2014	Literature
	Bensonomys	*gidleyi*	Baskin 1978	Literature
	Bensonomys	*yazhi*	Baskin 1978; ETMNH collection	Literature; specimens
	Bensonomys	*bradyi (gidleyi)*	ETMNH collection	Specimens
	Bensonomys	*arizonae*	Czaplewski 1987	Literature
	Bensonomys	*lindsayi*	Ronez et al. 2021	Literature
	Bensonomys	*hershkovitzi*	Martin, Goodwin et al. 2002	Literature
	Bensonomys	*meadensis*	Skinner & Hibbard 1972; Martin, Honey et al. 2002	Literature
?Sigmodontinae				
	Jacobsomys	*verdensis*	Czaplewski 1987; Ronez et al. 2021; ETMNH collection	Literature; specimens

	Jacobsomys	*dailyi*	Lindsay & Czaplewski 2011	Literature
	Jacobsomys	*dailyi*	May et al. 2011; Lindsay & Czaplewski 2011; Ronez et al. 2021	Literature
Neotominae				
	Peromyscus	*hagermensis*	Tomida 1985	Literature
	Peromyscus	sp. cf. *P. hagermanensis*	Albright 1999	Literature
	Peromyscus	*sarmocophinus*	Albright 1999	
	Peromyscus	sp. cf. *P. baumgartneri*	Albright 1999	Literature
	Peromyscus	*maximus*	Albright 1999	Literature
	Peromyscus	*leucopus*	ETMNH collection; USNM collection	Specimens
	Peromyscus	*maniculatus*	Lindsay 1972; ETMNH collection	Literature; specimens
	Peromyscus	*truei*	Lindsay 1972	Literature
	Peromyscus	sp.	UF collection	Specimens
	Neotomodon	*alstoni*	AMNH collection; Hoffeister 1945	Literature; specimens
	Neotomodon	*alstoni perotensis*	USNM collection	Specimens
	Neotoma (Paraneotoma)	*minutus*	Dalquest 1983	Literature
	Neotoma	*sawrockensis*	Hibbard 1967	Literature
	Neotoma	*fossilis*	Tomida 1985; AMNH collection	Literature; specimens
	Neotoma	*vaughani*	Korth 1990	Literature
	Neotoma	*taylori*	Tomida 1985; Zakrzewski 1991	Literature
	Paronychomys	*lemredfieldi*	Jacobs 1977; Kelly & Martin 2022	Literature
	Paronychomys	*tuttlei*	Jacobs 1977	Literature
	Paronychoms	*jacobsi*	Kelly 2013; Kelly & Martin 2022	Literature
	Xenomys	*nelsoni*	Cervante et al. 2016a	Literature
	Hodomys	*alleni*	Cervante et al. 2016b	Literature
Sigmodontinae				
	Zygodontomys	*brevicauda*	Solorzano et al. 2015	Literature
	Zygodontomys	sp.	Ronez et al. 2023	Literature

	Oligoryzomys	*fulvescens*	ETMNH collection	Specimens
	Oligoryzomys	*victus*	Turvery 2010	Literature
	Oryzomys	*palustris*	ETMNH collection; Hershkovitz 1971; Voss 2002	Literature; specimens
	Oryzomys	*gorgasi*	Hershkovitz 1971	Literature
	Oryzomys	*concolor*	Hershkovitz 1971	Literature
	Oryzomys	*capito*	Hershkovitz 1971	Literature
	Oryzomys	*megacephalus*	Weksler 2006	Literature
	Oryzomys	*macconnelli*	Weksler 2006	Literature

Appendix B: Measurements (mm) of GFS Specimens Examined in This Study

ETMNH Specimen Number	Material Type	Tooth Position	Side	Species	O-L	O-W	W/L
8218	isolated	M1	L	*Postcopemys* sp. large	2.47	1.8	0.73
8249	isolated	M1	L	*Postcopemys* sp. large	2.06	1.4	0.68
8250	isolated	M1	L	*Postcopemys* sp. large	2.07	1.35	0.65
8256	isolated	M1	R	*Postcopemys* sp. large	1.92	1.3	0.68
20554	isolated	M1	R	*Postcopemys* sp. large	2.03	1.3	0.64
20834	isolated	M1	L	*Postcopemys* sp. large	2.37	1.69	0.71
8202	isolated	M2	L	*Postcopemys* sp. large	1.93	1.67	0.87
16004	isolated	M2	L	*Postcopemys* sp. large	1.97	1.64	0.83
16005	isolated	M2	L	*Postcopemys* sp. large	2.03	1.8	0.89
32960	maxilla	M2	R	*Postcopemys* sp. large	2.04	1.71	0.84
32960	maxilla	M3	R	*Postcopemys* sp. large	1.38	1.38	1
20549	isolated	m1	R	*Postcopemys* sp. large	2.15	1.55	0.72
20557	isolated	m1	R	*Postcopemys* sp. large	2.2	1.65	0.75
8235	isolated	m1	R	*Postcopemys* sp. large	2.03	1.5	0.74
20551	isolated	m1	L	*Postcopemys* sp. large	2.16	1.48	0.69
13800	isolated	m1	L	*Postcopemys* sp. large	2.37	1.62	0.68
8212	isolated	m2	L	*Postcopemys* sp. large	1.97	1.72	0.87
16007	isolated	m2	R	*Postcopemys* sp. large	2.02	1.73	0.86
20552	isolated	m2	R	*Postcopemys* sp. large	2.04	1.78	0.87
26369	isolated	m2	L	*Postcopemys* sp. large	1.92	1.68	0.88
20549	isolated	m2	R	*Postcopemys* sp. large	1.87	1.59	0.85
14687	isolated	M2	L	*Postcopemys* sp. small	1.19	1.14	0.96
14888	maxilla	M2	R	*Postcopemys* sp. small	1.16	1.02	0.88
20525	maxilla	M2	R	*Postcopemys* sp. small	1.13	1.09	0.96
20555	isolated	M1	R	*Symmetrodontomys* sp.	1.7	1.13	0.66
8245	dentary	m1	L	*Symmetrodontomys* sp.	1.45	0.91	0.63
20485	dentary	m1	R	*Symmetrodontomys* sp.	1.53	0.95	0.62
8245	dentary	m2	L	*Symmetrodontomys* sp.	1.12	0.95	0.85
8245	dentary	m3	L	*Symmetrodontomys* sp.	1.13	0.83	0.73
32961	dentary	m1	R	Oryzomyini	1.8	1.17	0.65
32961	dentary	m2	R	Oryzomyini	1.45	1.28	0.88
32961	dentary	m3	R	Oryzomyini	1.4	1.15	0.82
20548	isolated	m1	L	*Peromyscus* sp.	1.48	0.91	0.61
20838	dentary	m1	L	*Peromyscus* sp.	1.4	0.91	0.65
12288	dentary	m1	L	*Peromyscus* sp.	1.38	0.86	0.62
8247	dentary	m1	L	*Peromyscus* sp.	1.57	1.01	0.64
20838	dentary	m2	L	*Peromyscus* sp.	1.08	0.89	0.82

12288	dentary	m2	L	*Peromyscus* sp.	1.13	0.93	0.82
8247	dentary	m2	L	*Peromyscus* sp.	1.22	1.07	0.88
36765	dentary	m2	L	*Peromyscus* sp.	1.46	1.21	0.83
36765	dentary	m3	L	*Peromyscus* sp.	1.28	1.02	0.8
8247	dentary	m3	L	*Peromyscus* sp.	1.17	0.89	0.76
8252	isolated	m3	R	*Peromyscus* sp.	1.1	0.88	0.8
20558	dentary	m3	L	*Peromyscus* sp.	1.02	0.81	0.79
788	maxilla	M1	L	*Neotomodon* sp.	1.47	1	0.68
25983	isolated	m1	R	*Neotomodon* sp.	1.54	1.08	0.7
16013	dentary	m1	R	*Neotomodon* sp.	1.79	1.28	0.72
8242	dentary	m1	L	*Neotomodon* sp.	1.67	0.97	0.58
8242	dentary	m2	L	*Neotomodon* sp.	1.36	1.13	0.83
8222	isolated	M1	L	*Neotoma* sp.	1.81	1.17	0.65
14697	isolated	M1	L	*Neotoma* sp.	1.89	1.34	0.71
24209	isolated	M1	R	*Neotoma* sp.	1.69	1.29	0.76
23634	maxilla	M1	L	*Neotoma* sp.	1.74	1.27	0.73
23634	maxilla	M1	R	*Neotoma* sp.	1.78	1.23	0.69
23634	maxilla	M2	L	*Neotoma* sp.	1.46	1.29	0.88
36765	maxilla	M2	R	*Neotoma* sp.	1.32	1.17	0.89
36766	isolated	m2	L	*Neotoma* sp.	1.72	1.2	0.7
36766	isolated	m2	L	*Neotoma* sp.	1.41	1.18	0.84
20595	dentary	m1	L	*Xenomys* sp.	1.51	0.89	0.59
14691	dentary	m1	L	*Xenomys* sp.	1.47	0.9	0.61
14691	dentary	m2	L	*Xenomys* sp.	1.12	0.91	0.82

Appendix C: List of Modern Cricetids in Tennessee. Information Is Acquired from Tennessee Wildlife Resource Agency: https://www.tn.gov/twra/wildlife/mammals/small.html

Subfamily	Genus	Species	Population
Neotominae			
	Reithrodontomys	*humulis*	uncommon
	Peromyscus	*maniculatus nubiterrae*	common
	Peromyscus	*leucopus*	common
	Peromyscus	*gossypinus*	common
	Ochrotomys	*nuttalli*	uncommon
	Neotoma	*floridana*	uncommon
	Neotoma	*magister*	uncommon
Sigmodontinae			
	Sigmodon	*hispidus*	common
	Oryzomys	*palustris*	common
Arvicolinae			
	Microtus	*chrotorrhinus*	uncommon
	Microtus	*ochrogaster*	common
	Microtus	*pennsylvanicus*	common
	Microtus	*pinetorum*	common
	Myodes	*gapperi*	common
	Ondatra	*zibethicus*	common
	Synaptomys	*cooperi*	uncommon

Appendix D: Character State Analysis of Upper Molars of <u>Postcopemys</u> sp. large from GFS and Other Comparable Taxa. GFS Species Is Highlighted in Bold

	M1										M2					
character state / specimen/taxon	cusp alternation: (0) opposite, (1) slightly alternate, with widely confluent dental fields of opposing cuspids, (2) more alternate, with limited overlap of dental fields of opposing cuspids, (3) strongly alternate, with distinct separation of dental fields of cuspids	bilobed anterocone: (0) absent, (1) present	parastyle: (0) absent, (1) present, isolated from anterocone, (2) present, closely attached to anterocone	prominent anterior cingulum descends from labial corner of anteroconid: (0) absent, (1) present but does not reach the protocone, (2) present and reach the protocone, enclosing the protoflexus	alignment of protolophule II and anterior arm of hypocone: (0) not aligned, (1) sub aligned, (2) aligned	mesoloph: (0) absent, (1) present, but not reaching the border of the tooth, (2) reaching the border of the tooth	mesostyle: (0) absent, (1) present	shelf-like hypoflexus: (0) absent, (1) present	direction of loph connections of the cuspids: (0) zigzagged, (1) relatively aligned with the midline of the tooth	posteroloph initially is separated from the metalophule by an enamel lake, but merges with metalophule and becomes posteroloph after wear: (0) absent, (1) present	anterior cingulid: (0) absent, (1) only extend labially or lingually, (2) has both lingual and labial arms	mesoloph: (0) absent, (1) present	alignment of the posterior arm of protoconid and entolophid: (0) not aligned, (1) sub aligned, (2) aligned	development of protoloph I: (0) absent, (1) present	development of isolated posteroloph: (0) absent, (1) present	reference
***Postcopemys* sp. large**	**2**	**0-1**	**1-2**	**1-2**	**0-1**	**1-2**	**0-1**	**0-1**	**1**	**1**	2	**1**	**0-1.5**	**1**	**1**	**GFS (this study)**
Postcopemys valensis	1	1	0	1	0.5	1	?	1	1	1	-	-	-	-	-	May et al. 2011
Postcopemys sp., cf. *P. valensis*	-	-	-	-	-	-	-	-	-	-	-	-	-	-	-	Kelly & Whistler 2014
Postcopemys vasquezi	1	1	?	1	0.5	1	1	0	1	?	1-2?	1	1	1	1	Jacobs 1977
Postcopemys repenningi	2	1-2	1	1	0	1	1	0	1	1	2	1	0	1	1	Lindsay & Czaplewski 2011
Postcopemys maxumensis	2	1-2	1	0-0.5	0	1	1	0	1	1	2	1	0	1	1	Lindsay & Czaplewski 2011
Postcopemys chapalensis	1	1	0	?	0	2	1	0	1	1	1	0-1	0	0	1	Rincón et al. 2016
Postcopemys sp. A	2	0.5	1	?	0	0	?	0.5	1	?	1-2?	0	0	0	1	Kelly 2013
Postcopemys sp. B	2	0.5	1	1?	0	1	0	0.5	1	?	2	1	0	0	1	Kelly 2013
Paronychomys lemredfieldi	1.5	1	?	0.5?	1	0	0	1	0	?	1	0-1	0	?	1?	Jacobs 1977 Kelly & Martin 2022
Paronychomys tuttlei	2	0	?	?	0.5	0	0	0	0.5	?	2	0	0	0	?	Jacobs 1977
Paronychomys jacobsi	2	0-1	0	1	1	0	0	0.5	0	?	1	0	1	0?	?	Kelly 2013 Kelly & Martin 2022

Appendix E: Character State Analysis of Lower Molars of Postcopemys sp. large from GFS and Other Comparable Taxa. GFS Species Is Highlighted in Bold

	m1								m2					
character state / specimen/taxon	lingual connection of anteroconid and metaconid: (0) absent, (1) present	anterolingual enamel margin between the anteroconid and metaconid: (0) no lingual connection between cuspids & metaflexid strongly present, (1) has lingual connection & metaflexid reduced to a groove differentiating the cuspids while creating a slightly concaved margin, (2) has lingual connection & no sign of metaflexid, a complete merge of two cuspids sharing smooth enamel margin	prominent anterior cingulid descends from labial corner of anteroconid: (0) absent, (1) present	connection between metaconid and protoconid: (0) absent, both cuspids join the anteroconid near its posteromedian margin and are not directly connected to one another (1) present, both cuspids join at around the midline before joining the anteroconid.	alignment of the posterior arm of protoconid and entolophid: (0) not aligned, (1) sub aligned, (2) aligned	mesolophid: (0) absent, (1) present, but not reaching the border of the tooth, (2) reaching the border of the tooth	direction of lophid connections of the cuspids: (0) zigzagged, (1) relatively aligned with the midline of the tooth	accessory cuspids or lophids (besides the mesolophid): (0) absent, (1) present	anterior cingulid: (0) absent, (1) present	mesolophid: (0) absent, (1) present	alignment of the posterior arm of protoconid and entolophid: (0) not aligned, (1) sub aligned, (2) aligned	direction of lophid connections of the cuspids: (0) zigzagged, (1) relatively aligned with the midline of the tooth	accessory cuspids or lophids: (0) absent, (1) present	reference
***Postcopemys* sp. large**	**0-1**	**0-2**	**1**	**0**	**1-2**	**0**	**1**	**0**	**1**	**0**	**0-2**	**1**	**0**	**GFS (this study)**
Postcopemys valensis	1	1	1	1	1	0	0	0	-	-	-	-	-	May et al. 2011
Postcopemys sp., cf. *P. valensis*	0	0	1	?	2	?	?	0-0.5	-	-	-	-	-	Kelly & Whistler 2014
Postcopemys vasquezi	?	?	1	1?	2	0	1	0	1	0	2	?	?	Jacobs 1977
Postcopemys repenningi	0	0	1	1	2	1	0.5	0	1	0-1	1	1	?	Lindsay & Czaplewski 2011
Postcopemys maxumensis	0	0	1	1	1	1	0	0	1	1	1	1	0?	Lindsay & Czaplewski 2011
Postcopemys chapalensis	0	0	1	1	0	1	1	1	1	1	1-2	1	1	Rincón et al. 2016
Postcopemys sp. A	0?	1	1	1	2	0	0	0	1	0	1	1	0	Kelly 2013
Postcopemys sp. B	0?	1	1	1	2	0	0	0	1	0	1	0	0	Kelly 2013
Paronychomys lemredfieldi	1	1	1	1	2	?	1	?	1	0	2	?	?	Jacobs 1977 Kelly & Martin 2022
Paronychomys tuttlei	1	1	?	?	?	?	?	?	1	?	2	?	?	Jacobs 1977
Paronychomys jacobsi	0-1	0-2	1	1	2	0	1	?	-	-	2	-	-	Kelly 2013 Kelly & Martin 2022

Appendix F: Character State Analysis of Upper M1 of Symmetrodontomys sp. from GFS and Other Comparable Taxa. GFS Species Is Highlighted in Bold

	M1													
character state / specimen/taxon	cusp alternation: (0) opposite, (1) slightly alternate, with widely confluent dental fields of opposing cuspids, (2) more alternate, with limited overlap of dental fields of opposing cuspids, (3) strongly alternate, with distinct separation of dental fields of cuspids	anterioconid bifurcation: (0) light, might disappear with wear, (1) strong and deep	conules of anterocone: (0) (sub-) equal size, (1) unequal, labial one is distinctly larger/taller	structure anterior to anterocone: (0) absent, (1) anterobasal stylar shelf is present, (2) anterobasal stylar shelf with anterostyle, (3) only has an anterostyle, no anterobasal stylar shelf	flexus shelf(s): (0) absent, (1) partially present (labial/lingual), (2) on both edges of tooth	flexus ridges (ridges that enclose the flexi): (0) absent, (1) present	parastyle: (0) absent, (1) present.	labial cingulum extends from the anterocone: (0) absent, (1) present but has no parastyle situated on it, (2) present with a parastyle	enamel lake formation: (0) absent, (1) present	mesoloph: (0) absent, (1) short, not reaching the border of tooth, (2) long and reaching	mesoloph placement: (0) absent, (1) close to paracone, (2) in the middle of the metaflexis	posterior cingulum: (0) absent, (1) present	rootlet: (0) absent, (1) present	reference
***Symmetrodontomys* sp.**	**1**	**1**	**1**	**2**	**1-2?**	**0**	**1**	**2**	**1**	**2**	**1**	**0**	**0**	**GFS (this study)**
Symmetrodontomys dammsi	0-1?	1	?	2	?	?	1	2	?	0?	?	?	?	Martin, Goodwin et al. 2002
Symmetrodontomys simplicidens	0	1	1	1-2?	1	0	1	2	1	2	1	1	?	Ronez et al. 2021
Jacobsomys dailyi	1	1	0-1	0	0	0	0-1	0-1	1	2	1	0-1	?	Lindsay & Czaplewski 2011 May et al. 2011 Ronez et al. 2021
Jacobsomys verdensis	0	1	0	1?	0-1	0	1	0-1	1	2	1	1	?	Ronez et al. 2021 Czaplewski 1987
Bensonomys meadensis	2	1	1	1	?	1	1	2	?	0	0	0	?	Skinner & Hibbard 1972
Bensonomys yazhi	2	0.5-1	0-1	1	1-2	0-1	0-1	0	0-1	0-1	0-1	0-1	1	Baskin 1978; ETMNH Collection (NAUQSP 2284)
Bensonomys gidleyi	2	1	1	1	1	1	0	0	?	1	1	1	1	Baskin 1978
Bensonomys bradyi (gidleyi) (NAUQSP 2283)	2	1	1	2	1	1	0	?	0	1	2	0.5	0	ETMNH Collection
Bensonomys arizonae	1	1	1	2-3	0?	0?	0-1	0-1?	?	0	0	0	0-1	Czaplewski 1987; ETMNH Coleection (NAUQSP 2285)
Bensonomys lindsayi	1	1	0	2	1	1	0	0	0	0-1?	0-1	0	?	Ronez et al. 2021

Appendix G: Character State Analysis of Lower Molars of Symmetrodontomys sp. from GFS And Other Comparable Taxa. GFS Species Is Highlighted in Bold

	dentary			m1									m2				m3			
character state / specimen/taxon	masseteric crest anterior end: (0) ridge-like, (1) knob-like	masseteric crest: (0) short and does not reach the anterior root of m1, (1) anteriorly ends beneath the anterior root of m1	mental foramen position on diastemal ramus: (0) labial, (1) dorsal	cusp alternation: (0)opposite, (1) slightly alternate, with broadly confluent dental fields of opposing cuspids, (2) more alternate, with limited overlap of dental fields of opposing cuspids, (3) strongly alternate, with distinct separation of dental fields of cuspids	anteroconid bifurcation: (0) light, might disappear with wear, (1) deep notch separating the lophulids	anterior mure: (0) super short and close to absent, tends to form an X-shaped (butterfly) pattern of wear between anterocond, metaconid and protoconid, (1) relatively long	anterior cingulum: (0) absent, (1) narrow, dental field does not connect with the anterocond field until heavy wear, (2) strongly present, dental field connect with the anteroconid	flexid shelf(s): (0) absent, (1) partially present (labial/lingual), (2) on both edges of tooth	protostylid: (0) absent, (1) present	ectostylid: (0) absent, (1) present	mesolophid: (0) absent, (1) present	posterior cingulum direction: (0) transversely, (1) posteriorly then lingually directed	cusp alternation: (0)opposite, (1) slightly alternate, with broadly confluent dental fields of opposing cuspids, (2) more alternate, with limited overlap of dental fields of opposing cuspids, (3) strongly alternate, with distinct separation of dental fields of cuspids	mesolophid: (0) absent, (1) present	rootlet: (0) absent, (1) present	anterior cingulum posterolabially directs towards the protoconid: (0) absent, (1) present, but not reaching, (2) reaching the protoconid	posterior cingulum inflated medially and forming a stylid: (0), (1) present	cusp alternation: (0) opposite, with dental field almost transversely present across labial and lingual cuspids, (1) slightly alternate, with dental field partially shared by opposite cusps, (2) more alternate, anterior side of labial cuspids opposite the posterior side of lingual cuspids, (3) strongly alternate, with distinct separation of dental fields of the cusps	rootlet: (0) absent, (1) present	the size of hypoconid and entoconid on m3: (0) not/slightly reduced, (1) greatly reduced	reference
***Symmetrodontomys* sp.**	**1**	**1**	**1**	**1**	**1**	**0**	**1**	**1**	**0**	**0**	**1**	**0-1**	**1**	**1**	**?**	**1**	**0**	**0**	**?**	**0**	**GFS (this study)**
Symmetrodontomys dammsi	1	1	1	1	1	0	1	1	0-1	0-1	0-1	1	0.5	0-1	?	2	?	0	?	0	Martin, Goodwin et al. 2002
Symmetrodontomys simplicidens	1	1	1	1	0-1	0	0-1	0-1	0	0	0-1	1	0	0	?	1?	?	0	?	0	Hibbard 1941 Ronez et al. 2021
Symmetrodontomys beckensis	1	1	1	3	0.5	0	0	?	1	1	0	1	0	0	?	2	?	0	?	0	Dalquest 1978
Jacobsomys dailyi	1	1	0	2	1	1	0-1	1	1	0	1	1	2	1	?	2	?	2	?	0	Lindsay & Czaplewski 2011; Ronez et al. 2021
Jacobsomys verdensis	-	-	-	1	1	0-0.5	1	0-1	0-1	1	1	0-1	-	1	-	2	-	-	-	-	Ronez et al. 2021; Czaplewski 1987; ETMNH Collection (NAUQSP 2287)
Bensonomys bradyi (gidleyi)	-	-	-	1	1	0.5	1	2	0	0	0	0	-	-	-	-	-	-	-		ETMNH Collection (NAUQSP 2283)
Bensonomys arizonae	?	1	1	1-2	0-1	1	1	0-1	0	0	0	0-1	1-2	0	?	2	0	0-1	?	0	ETMNH Collection (NAUQSP 2286); Czaplewski 1987
Bensonomys lindsayi	-	-	-	2	1	1	2	0.5	0	?	0	1	-	-	-	-	-	-	-	-	Ronez et al. 2021
Bensonomys sp.	-	-	-	1-2	1	1	1	?	1	0	1	0	1	1	?	1-2	0	0	?	0.5	Kelly & Whistler 2014
Bensonomys yazhi	-	-	-	2	1	1	0	2	0	0	0	0	1	?	1	2	1	?	1	1	Baskin 1978
Bensonomys gidleyi	-	-	-	2	1	1	1	2	0	0	0	1	?	0	1	1-2	1	?	1	1	Baskin 1978
Bensonomys hershkovitzi sp. nov.	1	1	1	2	0-1	0-1	1-2	1	0	0-1	1	1	-	-	-	-	-	-	-	-	Martin, Goodwin et al. 2002

Appendix H: Character State Analysis of Oryzomyini from GFS and Other Comparable Taxa. GFS Species Is Highlighted in Bold

	m1										m2								m3						
character state / specimens/taxon	cuspid alternation: (0) mainly opposite, (1) strongly opposite, (2) alternate	anteroconid (procingulum) bifurcation: (0) absent, (1) present	complete isolation of anteroconid (procingulum) from proto- and metaconid: (0) absent, (1) present	anterior cingulum from anteroconid: (0) absent, (1) present	ectolophid: (0) absent, (1) present	ectostylid: (0) absent, (1) present	mesolophid: (0) absent, (1) present	hypoflexid is deep and gets wider posteriorly: (0) absent, (1) present	posteroflexid: (0) enclosed, (1) mainly open	posterolophid (posterolophid) extends: (0) labially, (1) posteriorly	cuspid alternation: (0) mainly opposite (1) alternate	anterior cingulid extends from anteroconid: (0) absent, (1) present	mesostylid: (0) absent, (1) present	mesolophid: (0) absent, (1) present	ectoflexid: (0) absent, (1) present	hypoflexid is deep and gets wider posteriorly: (0) absent, (1) present	posteroflexid: (0) enclosed, (1) open	posterolophid (posterolophid) extends: (0) labially, (1)	dumbbell shape: (0) absent, (1) present	cuspid alternation: (0) mostly opposite, (1) alternate	narrow anterior cingulid: (0) absent, (1) present	merge of antoconid and hypoconid: (0) absent, (1) present	short but distinct posterior cingulid: (0) absent, (1) present	posterior ridge wrapping around posterior portion of the crown (from enotoconid to hypoconid): (0) absent, (1) present	reference
Oryzomyini (ETMNH 32961)	**0**	**0**	**0**	**1**	**1**	**0**	**0.5?**	**1**	**1**	**1**	**0**	**1**	**0**	**0**	**1**	**1**	**1**	**1**	**1**	**0**	**1**	**1**	**1**	**1**	**GFS (this study)**
Zygodontomys brevicauda	0	0	0	1	?	1	0	1	1	1	0	?	0	0	1	1	1	1	-	-	-	-	-	-	Solorzano et al. 2015
Zygodontomys sp.	-	-	-	-	-	-	-	-	-	-	0	1	1	0	1	1	1	1	-	-	-	-	-	-	Ronez 2023
Oligoryzomys fulvescens	1	0.5	1	1	0	0	0?	1	0	0	0	1	0	0?	0	0.5	0	0	0	0	0	1	0	0	ETMNH collection
Oligoryzomys victus	1	0	0	1	1	?	1	0	1	1	0	1	0	1	0	0	1	1	1	0	1	1	0	0	Turvery 2010
Oryzomys palustris	1	0	0	1	1	1	0?-1	1	0-1	0-1	0	1	0-1	1?	1	1	0-1	1	0-0.5	0	1	0.5-1	0	0	Hershkovitz 1971; Voss 2002; ETMNH collection
Oryzomys gorgasi	1	1	0	1	0	0	1	0	0	0	0	1	?	1	1?	0	0	0	0	0	?	1	0	0	Hershkovitz 1971
Oryzomys concolor	0	0	1	0?	1?	0	1	0.5	0	0	0	1	?	1	?	0.5	0	0	0	0	1	1	0	0	Hershkovitz 1971
Oryzomys capito	0	0	0	1	1	1	1	1	0	0	0	1?	?	1	1	0	0	0	0	0	1	1	0	0	Hershkovitz 1971
Oryzomys megacephalus	1	0	0	1	1	1	1	0.5	1	0	0	1	0	1	0	0	0	0	0	0	1	1	0	0	Weksler 2006
Oryzomys macconnelli	1	1	0	0	1	1	1	0.5	0	0	0	1	0	1	1	0	0	0	0	0	1	1	0	0	Weksler 2006

Appendix I: Character State Analysis of <u>Peromyscus</u> sp. from GFS and Other Comparable Taxa. GFS Species Is Highlighted in Bold

	dentary			m1						m2				m3			
character state / specimen/taxon	masseteric crest anterior end: (0) ridge-like, (1) knob-like	masseteric crest: (0) short and does not reach the anterior root of m1, (1) anteriorly ends beneath the anterior root of m1	mental foramen position on diastemal ramus: (0) labial, (1) dorsal	cusp alternation: (0)opposite, (1) slightly alternate, with broadly confluent dental fields of opposing cuspids, (2) more alternate, with limited overlap of dental fields of opposing cuspids, (3) strongly alternate, with distinct separation of dental fields of cuspids	anteroconid bifurcation: (0) absent, (1) light, might disappear with wear, (2) deep notch separating the lophulids	anterior cingulum: (0) absent, (1) present	flexid ridge: (0) absent, (1) present	ectostylid: (0) absent, (1) present	mesolophid: (0) absent, (1) does not reach the tooth border, (2) reach the tooth border	cusp alternation: (0)opposite, (1) slightly alternate, with broadly confluent dental fields of opposing cuspids, (2) more alternate, with limited overlap of dental fields of opposing cuspids, (3) strongly alternate, with distinct separation of dental fields of cuspids	flexid ridge: (0) absent, (1) present	mesolophid: (0) absent, (1) present	anterior cingulum posterolingually directs towards the protoconid: (0) absent, (1) present	cusp alternation: (0) opposite, with dental field almost transversely present across labial and lingual cuspids, (1) slightly alternate, with dental field partially shared by opposite cusps, (2) more alternate, anterior side of labial cuspids opposite the posterior side of lingual cuspids, (3) strongly alternate, with distinct separation of dental fields of the cusps	flexid ridge: (0) absent, (1) present	the size of hypoconid and entoconid on m3: (0) not/slightly reduced, (1) greatly reduced	reference
***Peromyscus* sp.**	**0-1**	**1**	**1**	**1-2**	**0**	**1**	**0-0.5**	**0**	**0-1**	**0-1**	**0-0.5**	**0-1**	**1**	**0-2**	**0-1**	**0-1**	**GFS (this study)**
Peromyscus	-	-	-	1-2	0-2	1	0-1	0-1?	2	2	0	0	1	0	1?	1	UF collection
Peromyscus hagermanensis	1	1	1	1	0-1	1	1	0-1	0-2	1?	1	1	1	0	1	0.5?	Hibbard 1962; Tomida 1985; Mou 2011
Peromyscus sp. cf. *P. hagermanensis*	-	-	-	2	0	1	1	0	0	1	?	0	1	-	-	-	Albright 1999
Peromyscus sarmocophinus	-	-	-	2	1	1	0	0-1	2	1	0	1	1	?	?	0.5?	Albright 1999

VITA

ZIQI (STOKKE) XU

Education:	M.S. Geosciences, East Tennessee State University, Johnson City, Tennessee, 2023
	B.A. Earth and Space Sciences, East Tennessee State University, Johnson City, Tennessee, 2019
Professional Experience:	Graduate Assistant, East Tennessee State University, College of Arts and Sciences, 2021-2023
	Teaching Assistant, East Tennessee State University, College of Arts and Sciences, 2022-2023
Honors and Awards:	Carolyn K. Dupuy Memorial Scholarship, Center of Excellence in Paleontology, 2023 & 2022
	Collins Chew Research Award, East Tennessee State University, 2022